

Article

Sulfated Triterpene Glycosides from the Far Eastern Sea Cucumber *Cucumaria djakonovi*: Djakonoviosides C₁, D₁, E₁, and F₁; Cytotoxicity against Human Breast Cancer Cell Lines; Quantitative Structure–Activity Relationships

Alexandra S. Silchenko ^{1,*}, Anatoly I. Kalinovsky ¹, Sergey A. Avilov ¹, Roman S. Popov ¹, Ekaterina A. Chingizova ¹, Ekaterina S. Menchinskaya ¹, Elena A. Zelepuga ¹, Elena G. Panina ², Vadim G. Stepanov ², Vladimir I. Kalinin ¹ and Pavel S. Dmitrenok ^{1,*}

- ¹ G.B. Elyakov Pacific Institute of Bioorganic Chemistry, Far Eastern Branch of the Russian Academy of Sciences, Pr. 100-letya Vladivostoka 159, 690022 Vladivostok, Russia; kaaniv@piboc.dvo.ru (A.I.K.); avilov_sa@piboc.dvo.ru (S.A.A.); popov_rs@piboc.dvo.ru (R.S.P.); chingizova_ea@piboc.dvo.ru (E.A.C.); ekaterinamenchinskaya@gmail.com (E.S.M.); zel@piboc.dvo.ru (E.A.Z.); kalininv@piboc.dvo.ru (V.I.K.)
- ² Kamchatka Branch of Pacific Institute of Geography, Far Eastern Branch of the Russian Academy of Sciences, Partizanskaya st. 6, 683000 Petropavlovsk-Kamchatsky, Russia; egpanina777@gmail.com (E.G.P.); stepanovvadim24@gmail.com (V.G.S.)
- * Correspondence: silchenko_als@piboc.dvo.ru (A.S.S.); paveldmt@piboc.dvo.ru (P.S.D.); Tel./Fax: +7-(423)2-31-40-50 (A.S.S. & P.S.D.)



Citation: Silchenko, A.S.; Kalinovsky, A.I.; Avilov, S.A.; Popov, R.S.; Chingizova, E.A.; Menchinskaya, E.S.; Zelepuga, E.A.; Panina, E.G.; Stepanov, V.G.; Kalinin, V.I.; et al. Sulfated Triterpene Glycosides from the Far Eastern Sea Cucumber *Cucumaria djakonovi*: Djakonoviosides C₁, D₁, E₁, and F₁; Cytotoxicity against Human Breast Cancer Cell Lines; Quantitative Structure–Activity Relationships. *Mar. Drugs* **2023**, *21*, 602. <https://doi.org/10.3390/md21120602>

Academic Editors: Bae Munhyung and Jae-hyuk Jang

Received: 3 November 2023

Revised: 20 November 2023

Accepted: 21 November 2023

Published: 22 November 2023



Copyright: © 2023 by the authors. Licensee MDPI, Basel, Switzerland. This article is an open access article distributed under the terms and conditions of the Creative Commons Attribution (CC BY) license (<https://creativecommons.org/licenses/by/4.0/>).

Abstract: Four new mono- and trisulfated triterpene penta- and tetraosides, djakonoviosides C₁ (1), D₁ (2), E₁ (3), and F₁ (4) were isolated from the Far Eastern sea cucumber *Cucumaria djakonovi* (Cucumariidae, Dendrochirotida), along with six known glycosides found earlier in other *Cucumaria* species. The structures of unreported compounds were established on the basis of extensive analysis of 1D and 2D NMR spectra as well as by HR-ESI-MS data. The set of compounds contains six different types of carbohydrate chains including two new ones. Thus, djakonovioside C₁ (1) is characterized by xylose as the second residue, that was a branchpoint in the pentasaccharide chain. Meanwhile, only quinovose and rarely glucose have been found earlier in pentasaccharide chains branched at C-2 of the second sugar unit. Djakonovioside E₁ (3) is characterized by a tetrasaccharide trisulfated chain, with glucose as the second residue. So, in the series of isolated glycosides, three types of sugars in the second position were presented: the most common, quinovose—in six compounds; glucose—in three substances; and the rare xylose—in one glycoside. The set of aglycones was composed of holostane- and non-holostane-type polycyclic systems; the latter comprised normal and reduced side chains. Noticeably, isokoreoside A (9), isolated from *C. djakonovi*, was a single glycoside having a 9(11)-double bond, indicating two oxidosqualenecyclases are operating in the process of the biosynthesis of aglycones. Some of the glycosides from *C. djakonovi*, which were characterized by pentasaccharide branched chains containing one to three sulfate groups, are chemotaxonomic features of the representatives of the genus *Cucumaria*. The assortment of sugar parts of *Cucumaria*'s glycosides was broadened with previously undescribed penta- and tetrasaccharide moieties. The metabolic network of sugar parts and aglycones is constructed based on biogenetic relationships. The cytotoxic action of compounds 1–10, isolated from *C. djakonovi*, against human breast cancer cell lines was investigated along with the hemolytic activity. Erythrocytes were, as usual, more sensitive to the membranolytic action of the glycosides than cancer cells. The triple-negative breast cancer MDA-MB-231 cell line was more vulnerable to the action of glycosides in comparison with the other tested cancer cells, while the MCF-7 cell line was less susceptible to cytotoxic action. Djakonovioside E₁ (3) demonstrated selective action against ER-positive MCF-7 and triple-negative MDA-MB-231 cell lines, while the toxic effect in relation to normal mammary epithelial cells (MCF-10A) was absent. Cucumarioside A₂-5 (6) inhibited the formation and growth of colonies of cancer cells to 44% and tumor cell migration to 85% of the control. Quantitative structure–activity relationships (QSAR) were calculated on the basis of the correlational analysis of the physicochemical properties and structural

features of the glycosidic molecules and their membranolytic activity. QSAR revealed the extremely complex nature of such relationships, but these calculations correlated well with the observed SAR.

Keywords: *Cucumaria djakonovi*; Dendrochirotida; triterpene glycosides; djakonoviosides; sea cucumber; hemolytic and cytotoxic activity; human breast cancer; QSAR

1. Introduction

Sea cucumbers are marine invertebrates belonging to the class Holothuroidea of the phylum Echinodermata. They have wide distributions in all the oceans from shallow waters to significant depths. Sea cucumbers are mainly detritophages, collecting food from superficial sediments through their tentacles. The representatives of the order Dendrochirotida, including *Cucumaria djakonovi*, are filtrators, i.e., they filter solid particles dispersed in sea water also using their branched tentacles. For this reason, sea cucumbers have great importance for the ecosystem, providing a sort of cleaning service by recycling and decomposing the substrate. Nowadays, a growing number of marine organisms are being chemically investigated in the search for new biomolecules with pharmacological potential. Sea cucumbers are among them because they produce specific metabolites, triterpene glycosides, which are uncommon in the animal kingdom. Investigations of the triterpene glycosides of diverse representatives of the class Holothuroidea have a long history, beginning from structural studies of the artifact genines obtained as a result of acid hydrolysis, followed by the structure establishment of native compounds [1,2]. The continuation of these researches resulted in the appearance of the modern approaches of the separation of complex mixtures of native metabolites giving individual glycosides, including minor ones, possessing unique structural features [3,4]. All these broaden the fundamental knowledge about the chemical diversity of natural products in general and of triterpenoids and their derivatives in particular. Actually, each new research study of the glycosidic composition of previously uninvestigated species or reinvestigation of species that were previously studied, but using modern techniques and equipment, leads to the finding of novel compounds [4,5]. Fairly recently, the metabolomic studies of the glycosidic profiles of diverse species of holothuroids appeared, providing very useful data on the chemical diversity of glycosides, their distribution, and their content inside the different internal parts of animals, as well as their ecological signal functions [6–10]. The interest of researchers in glycosides has been increased by their diverse and unique biological activity, including anticancer activity against different types of tumors, and immunomodulatory properties [11–13]. Hence, some of these substances isolated from *C. djakonovi* demonstrated a promising action against human breast cancer cells, especially against the most aggressive triple-negative MDA-MB-231 cell line, suppressing cells' viability, inhibiting colony formation and growth, and inhibiting the migration of cells [5]. These data indicate that glycosides could be used in the target therapy of breast cancer. An additional direction of scientific interest in these metabolites, based on the use of them as chemotaxonomic markers, allows for defining the systematic position and resolving taxonomic issues by analysis of the structural features of glycosides. Particularly, on the one hand, the isolation of novel compounds from *C. djakonovi* corroborated the apartness of this species from other closely related *Cucumaria* species; on the other hand, the presence of the same compounds in different species of the genus *Cucumaria* confirmed the specificity of glycosides at the genus level [5,14]. The analysis of the structure–activity relationships of these metabolites shows the significance of the different parts of molecules for the demonstration of bioactivity and their influence on the mechanisms of action of glycosides [15]. The accumulation of such data provides the opportunity to predict glycosides' bioactivity. So, the calculations of the quantitative structure–activity relationships (QSAR) for the glycosides from *C. djakonovi* are one of the first steps in this prospective direction. As data are accumulated, the combinatorial libraries of glycosides are formed and expanded, and, on the basis of

the structural biogenetic rows of aglycones and the carbohydrate chains of glycosides, the pathways of biosynthesis could be traced [4], revealing the sequence of enzymes acting during the formation of glycosides, which is necessary for the regulation of the biosynthesis of these promising compounds in the future.

As a continuation of the study of the glycosides of *C. djakonovi* collected in Avacha Gulf, the isolation, structure elucidation, and biological activity testing of a series of new triterpene glycosides, djakonoviosides C₁ (1), D₁ (2), E₁ (3), and F₁ (4), and several known compounds were reported. The chemical structures of 1–4 were elucidated by the analyses of the ¹H, ¹³C NMR, 1D TOCSY, and 2D NMR (¹H,¹H COSY, HMBC, HSQC, ROESY) spectra as well as the HR-ESI mass spectra. All the original spectra are displayed in Figures S1–S57 in the Supplementary Materials. The hemolytic activity against human erythrocytes and the cytotoxicity against human breast cancer cell lines MCF-7, T-47D, and triple-negative MDA-MB-231, as well as the non-tumor mammary epithelial cell line MCF-10A, were studied. QSAR analysis was conducted for the series of 20 triterpene glycosides found in *C. djakonovi*.

2. Results

2.1. Structure Elucidation of Glycosides

The crude glycosidic sum of *Cucumaria djakonovi* (1.379 g) was obtained after the hydrophobic chromatography of the concentrated ethanolic extract on a Polychrom-1 column (powdered Teflon, Biolar, Latvia). Then, it was chromatographed on Si gel columns (CC) with the stepped gradient of the eluents system of CHCl₃/EtOH/H₂O, in ratios of 100:50:4, 100:75:10, 100:100:17, and 100:125:25, and five fractions were obtained. The fractions 3–5, isolated after the repeated CC with the system of eluents CHCl₃/EtOH/H₂O (100:75:10), (100:100:17), and (100:125:25), were subsequently submitted to HPLC on reversed-phase semipreparative columns, Phenomenex Synergi Fusion RP (10 × 250 mm) and Synergi Hydro RP (10 × 250 mm), as well as chiral analytical column Kromasil 3-Cellucoat RP (4.6 × 150 mm), to give 10 individual novel and known glycosides (Figure 1).

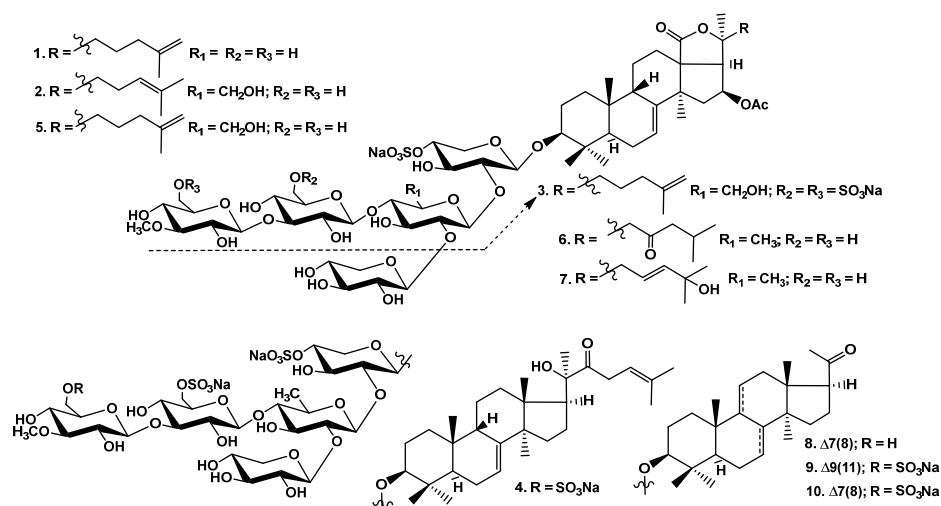


Figure 1. Chemical structures of glycosides of *Cucumaria djakonovi*: 1—djakonovioside C₁; 2—djakonovioside D₁; 3—djakonovioside E₁; 4—djakonovioside F₁; 5—okhotoside A₂-1; 6—cumucarioside A₂-5; 7—frondoside A₂-3; 8—cumucarioside A₃-2; 9—iskoreoside A; 10—koreoside A.

The sugar configurations in glycosides 1–4 were assigned as *D* on the basis of an analogy with all other known triterpene glycosides from sea cucumbers.

The molecular formula of djakonovioside C₁ (1) was determined to be C₆₀H₉₃O₃₀SNa from the [M_{Na} – Na][−] ion peak at *m/z* 1325.5451 (calc. 1325.5478) in the (−)HR-ESI-MS (Figure S8). The structures of the identical aglycone moieties of djakonoviosides C₁ (1) and E₁ (3) and okhotoside A₂-1 (5) were established by the analysis of their NMR spectra (Table 1,

(Tables S1 and S2; Figures S1–S6, S17–S22, and S33–S38). The holostane-type aglycone (characteristic signals of 18(20)-lactone were observed at δ_C 180.2 (C-18) and 85.5 (C-20)) contains 7(8)- (the signals of CH-7 at δ_C 120.2 and δ_H 5.57 (m) and C-8 at δ_C 145.5) and 25(26)-double bonds (the signals of C-25 at δ_C 145.4 and CH₂-26 at δ_C 110.8 and δ_H 4.72 (m)) and 16 β -acetoxy group (the signals at δ_C 75.3 (C-16), 170.7 (OCOCH₃), and 21.2 (OCOCH₃). The orientation of this substituent was confirmed by the NOE correlation between H-16 and H-32 as well as by the value of the coupling constant ($J_{16/17} = 8.7$ Hz) [16].

Table 1. ¹³C and ¹H NMR chemical shifts and HMBC and ROESY correlations of the aglycone moiety of djakonovioside C₁ (**1**).

Position	δ_C mult. ^a	δ_H mult. (<i>J</i> in Hz) ^b	HMBC	ROESY
1	35.9 CH ₂	1.31 m		H-3, H-11, H-19
2	26.8 CH ₂	1.95 m		
		1.78 m		H-19, H-30
3	88.8 CH	3.20 dd (4.7; 12.1)		H-1, H-5, H-31, H1-Xyl1
4	39.3 C			
5	47.9 CH	0.91 dd (4.7; 10.7)	C: 19	H-1, H-3, H-31
6	23.1 CH ₂	1.91 m		H-19, H-30, H-31
7	120.2 CH	5.57 m		H-15, H-32
8	145.5 C			
9	47.0 CH	3.30 brd (14.1)		H-19
10	35.3 C			
11	22.4 CH ₂	1.72 m		H-1
		1.47 m		H-32
12	31.2 CH ₂	2.10 m		H-17, H-21, H-32
13	59.3 C			
14	47.3 C			
15	43.5 CH ₂	2.54 dd (7.4; 12.1)	C: 13, 17, 32	H-7, H-32
		1.61 dd (8.7; 12.1)		
16	75.3 CH	5.82 dd (8.7; 16.1)		H-32
17	54.5 CH	2.66 d (8.7)	C: 12, 13, 18, 21	H-12, H-16, H-21, H-32
18	180.2 C			
19	23.8 CH ₃	1.06 s	C: 5, 9, 10	H-1, H-2, H-6, H-9
20	85.5 C			
21	28.0 CH ₃	1.51 s	C: 17, 20, 22	H-12, H-17, H-22
22	38.2 CH	2.25 td (4.7; 12.7)		
		1.80 m		H-21
23	22.9 CH ₂	1.47 m		
		1.35 m		
24	38.1 CH ₂	1.91 m		
25	145.4 C			
26	110.8 CH ₂	4.72 m	C: 24, 27	H-24
27	22.0 CH ₃	1.65 s	C: 24, 25, 26	
30	17.1 CH ₃	1.01 s	C: 3, 4, 5, 31	H-2, H-6, H-31
31	28.4 CH ₃	1.17 s	C: 3, 4, 5, 30	H-3, H-5, H-6, H-30, H-1 Xyl1
32	32.1 CH ₃	1.15 s	C: 8, 13, 14, 15	H-7, H-12, H-15, H-16, H-17
OCOCH ₃	170.7 C			
OCOCH ₃	21.2 CH ₃	2.01 s	OAc	OAc

^a Recorded at 125.67 MHz in C₅D₅N/D₂O (4/1). ^b Recorded at 500.12 MHz in C₅D₅N/D₂O (4/1). The original spectra of **1** are provided in Figures S1–S7.

Extensive analysis of the ¹H, ¹³C NMR, and HSQC spectra of the carbohydrate moiety of djakonovioside C₁ (**1**) (Table 2; Figures S1–S7) indicated the presence of the pentasaccharide chain with β -glycosidic bonds because five doublets of the anomeric protons at δ_H 4.73–5.25 ($J = 6.8$ – 8.0 Hz) and the signals of the corresponding anomeric carbons at δ_C 102.4–105.6 were observed. Analysis of the ¹H, ¹H COSY, and 1D TOCSY spectra of each monosaccharide residue started from the anomeric proton, followed by ROESY and HSQC correlations analyses, allowed to determine the monosaccharide composition and

the positions of glycosidic bonds. Hence, it was found that the second sugar in the chain is the xylose residue (Xyl2) that is linked to the Xyl1 residue at C-2. The second sugar unit (Xyl2) is bound with another two monosaccharides, being a branchpoint of the chain. The third monosaccharide unit—Glc3—was attached to C-4 Xyl2, and the additional xylose residue (Xyl5) was attached to C-2 Xyl2, causing glycosylation effects ($\delta_{C-4\text{Xyl2}}$ 77.9 and $\delta_{C-2\text{Xyl2}}$ 82.6). The analysis of the NMR spectra showed that 3-O-methylglucose (MeGlc4) was a terminal monosaccharide unit linked to C-3 Glc3. The positions of the glycosidic linkages were corroborated by the ROESY and HMBC correlations between the H-1 Xyl1 and H-3 (C-3) of the aglycone, H-1 Xyl2 and H-2 (C-2) Xyl1, H-1 Glc3 and H-4 (C-4) Xyl2, H-1 MeGlc4 and H-3 (C-3) Glc3, and H-1 Xyl5 and H-2 (C-2) Xyl2 (Table 2). The single sulfate group was attached to the C-4 Xyl1, causing an α -shifting effect of its signal to δ_C 76.1, instead of the δ_C ~70 observed in non-sulfated compounds.

Table 2. ^{13}C and ^1H NMR chemical shifts and HMBC and ROESY correlations of carbohydrate moiety of djakonovioside C_1 (**1**).

Atom	δ_C mult. ^a	δ_H mult. (J in Hz) ^{b,c,d}	HMBC	ROESY
Xyl1 (1→C-3)				
1	104.7 CH	4.73 d (7.5)	C: 3	H-3; H-3, 5 Xyl1
2	81.2 CH	3.97 t (8.8)	C: 1 Xyl2; C: 1 Xyl1	H-1 Xyl2
3	75.3 CH	4.30 t (8.8)	C: 2, 4 Xyl1	H-1 Xyl1
4	76.1 CH	5.02 m		H-2 Xyl1
5	64.2 CH ₂	4.80 dd (4.8; 11.0) 3.85 dd (8.8; 11.0)	C: 1, 3 Xyl1	H-1 Xyl1
Xyl2 (1→2Xyl1)				
1	102.7 CH	5.25 d (6.8)	C: 2 Xyl1	H-2 Xyl1; H-3, 5 Xyl2
2	82.6 CH	3.95 dd (6.8; 8.9)	C: 1 Xyl2; C: 1 Xyl5	H-1 Xyl5
3	74.7 CH	4.12 t (8.9)	C: 4 Xyl2	H-1 Xyl2
4	77.9 CH	4.19 m	C: 1 Glc3	H-1 Glc3
5	63.7 CH ₂	4.39 dd (5.3; 11.3) 3.55 dd (9.0; 11.3)		H-1 Xyl2
Glc3 (1→4Xyl2)				
1	102.4 CH	4.85 d (7.5)	C: 4 Xyl2	H-4 Xyl2; H-3, 5 Glc3
2	73.3 CH	3.90 t (9.0)	C: 1 Glc3	
3	86.8 CH	4.15 t (9.0)	C: 2, 4 Glc3; C: 1 MeGlc4	H-1 MeGlc4; H-1, 5 Glc3
4	69.3 CH	3.88 t (9.0)	C: 3, 5 Glc3	
5	77.2 CH	3.80 m		
6	61.6 CH ₂	4.26 dd (3.0; 11.3) 4.02 dd (6.0; 11.3)	C: 5 Glc3	H-1 Glc3
MeGlc4 (1→3Glc3)				
1	104.6 CH	5.19 d (8.0)	C: 3 Glc3	H-3 Glc3; H-3, 5 MeGlc4
2	74.6 CH	3.85 t (8.8)	C: 1, 3 MeGlc4	
3	87.0 CH	3.67 t (8.8)	C: 2, 4 MeGlc4; OMe	H-1 MeGlc4; OMe
4	70.4 CH	3.88 t (8.8)		
5	77.5 CH	3.92 m		H-1 MeGlc4
6	61.7 CH ₂	4.37 dd (3.2; 12.0) 4.04 dd (6.4; 12.0)		
OMe	60.7 CH ₃	3.80 s	C: 3 MeGlc4	
Xyl5 (1→2Xyl2)				
1	105.6 CH	5.09 d (7.2)	C: 2 Xyl2	H-2 Xyl2; H-3, 5 Xyl5
2	74.8 CH	3.91 t (8.8)	C: 1, 3 Xyl5	
3	76.6 CH	4.01 t (8.8)	C: 2, 4 Xyl5	H-1 Xyl5
4	70.0 CH	4.07 m		
5	66.5 CH ₂	4.28 dd (5.6; 12.0) 3.56 t (10.4)	C: 3, 4 Xyl5 C: 3, 4 Xyl5	H-1 Xyl5

^a Recorded at 125.67 MHz in C₅D₅N/D₂O. ^b Bold—interglycosidic positions. ^c Italics—sulfate position. ^d Recorded at 500.12 MHz in C₅D₅N/D₂O. Multiplicity by 1D TOCSY. The original spectra of **1** are provided in Figures S1–S7.

The (−)ESI-MS/MS of **1** (Figure S8) demonstrated the fragmentation of the $[M_{Na} - Na]^-$ ion, with m/z 1325.5 giving fragment ion peaks at m/z 1265.5 $[M_{Na} - Na - CH_3COOH]^-$, 1223.5 $[M_{Na} - Na - NaSO_3 + H]^-$, 1193.5 $[M_{Na} - Na - Xyl]^-$, 987.4 $[M_{Na} - Na - MeGlc - Glc + H]^-$, 813.2 $[M_{Na} - Na - Agl - H]^-$, 681.1 $[M_{Na} - Na - Agl - Xyl]^-$, and 595.2 $[M_{Na} - Na - Agl - XylSO_3]^-$. The (+)ESI-MS/MS of **1** demonstrated the fragmentation of the $[M_{Na} + Na]^+$ ion, with m/z 1371.5 leading to ion peaks with m/z 1251.6 $[M_{Na} + Na - NaHSO_4]^+$ and 1179.6 $[M_{Na} + Na - MeGlc + H]^+$.

These data indicate that djakonovioside C₁ (**1**) is 3β-O-(3-O-methyl-β-D-glucopyranosyl-(1→3)-β-D-glucopyranosyl-(1→4)-[(1→2)-β-D-xylopyranosyl]-β-D-xylopyranosyl-(1→2)-4-O-sodium sulfate-β-D-xylopyranosyl)-16β-acetoxylholosta-7,25-dien.

The molecular formula of djakonovioside D₁ (**2**) was determined as C₆₁H₉₅O₃₁SNa from the $[M_{Na} - Na]^-$ ion peak at m/z 1355.5596 (calc. 1355.5584) and the $[M_{Na} - Na - H]^2^-$ ion peak at m/z 677.2767 (calc. 677.2755) in the (−)HR-ESI-MS (Figure S16). The aglycone of djakonovioside D₁ (**2**) (Table 3, Figures S9–S15) was structurally close to that of **1**, only differing by the position of the double bond in the side chain. So, all the signals of the polycyclic nuclei in the NMR spectra of **2** and **1** were almost coincident. The signals of the side chain were assigned by the analysis of the NMR spectra of **2**: an isolated spin system formed by the protons from H-22 to H-24 was found in the ¹H,¹H COSY spectrum, and the characteristic signals in the ¹³C and ¹H NMR spectra at δ_C 123.9 (C-24), δ_H 5.00 (m, H-24) and 132.1 (C-25) corresponded to the 24(25)-double bond. Its position was confirmed by the correlations H-26(27)/C: 24, 25, 27(26) in the HMBC spectrum.

Table 3. ¹³C and ¹H NMR chemical shifts and HMBC and ROESY correlations of aglycone moiety of djakonovioside D₁ (**2**).

Position	δ _C mult. ^a	δ _H mult. (J in Hz) ^b	HMBC	ROESY
1	35.9 CH ₂	1.29 m		H-11
2	26.7 CH ₂	1.93 m 1.85 m		
3	89.2 CH	3.21 dd (3.9; 11.6)		H-5, H1-Xyl1
4	39.4 C			
5	47.8 CH	0.89 dd (5.2; 11.3)	C: 6, 10, 19, 30	H-3, H-31
6	23.0 CH ₂	1.88 m		H-30, H-31
7	120.2 CH	5.58 m		H-15
8	145.5 C			
9	47.0 CH	3.29 brd (14.6)		H-19
10	35.3 C			
11	22.4 CH ₂	1.72 m 1.48 m		H-1
12	31.2 CH ₂	2.10 m		H-21
13	59.3 C			
14	47.3 C			
15	43.5 CH ₂	2.57 dd (7.5; 12.0) 1.61 m	C: 13, 17, 32	H-7
16	75.2 CH	5.85 dd (8.2; 16.7)		H-32
17	54.3 CH	2.70 d (8.2)	C: 12, 13, 18, 21	H-32
18	180.2 C			
19	23.7 CH ₃	1.06 s	C: 5, 9, 10	H-2, H-6, H-9
20	85.5 C			
21	28.0 CH ₃	1.56 s	C: 17, 20, 22	H-12, H-17, H-23
22	38.5 CH	2.42 td (4.1; 12.3) 1.83 m		
23	23.5 CH ₂	2.03 m 1.91 m		
24	123.9 CH	5.00 m		
25	132.1 C			
26	25.4 CH ₃	1.60 s	C: 24, 25, 27	H-24

Table 3. Cont.

Position	δ_C mult. ^a	δ_H mult. (J in Hz) ^b	HMBC	ROESY
27	17.6 CH ₃	1.54 s	C: 24, 25, 26	
30	17.2 CH ₃	1.05 s	C: 3, 4, 5, 31	H-2, H-6, H-31
31	28.5 CH ₃	1.18 s	C: 3, 4, 5, 30	H-3, H-30, H-1 Xyl1
32	32.1 CH ₃	1.17 s	C: 8, 13, 14, 15	H-15, H-16, H-17
OCOCH ₃	170.7 C			
OCOCH ₃	21.0 CH ₃	1.97 s	OAc	OAc

^a Recorded at 125.67 MHz in C₅D₅N/D₂O. ^b Recorded at 500.12 MHz in C₅D₅N/D₂O. The original spectra of 2 are provided in Figures S9–S15.

Extensive analysis of the ¹H, ¹³C NMR, ¹H, ¹H COSY, 1D TOCSY, HSQC, and ROESY spectra of the carbohydrate part of djakonovioside D₁ (2) and okhtoside A₂-1 (5) (Tables 4 and S3; Figures S9–S15 and S33–S38) revealed the presence of the same monosulphated pentasaccharide chains. The typical signals for quinovose residue were absent, while three signals characteristic for the hydroxymethylene groups of glucopyranose residues at δ_C 61.4, 61.1, and 61.7 were observed. Further analysis of the sugar composition and sequence, as well as the glycosidic bond positions, showed that the second and third units in the chain were glucose residues (Glc2 and Glc3); the 3-O-methylglucose (MeGlc4) and xylose (Xyl5) residues were terminal, forming a carbohydrate chain branched by C-2 Glc2. A sulphate group was attached to C-4 Xyl1 (δ_C 76.1), as in djakonovioside C₁ (1).

Table 4. ¹³C and ¹H NMR chemical shifts and HMBC and ROESY correlations of carbohydrate moiety of djakonovioside D₁ (2).

Atom	δ_C mult. ^a	δ_H mult. (J in Hz) ^{b,c,d}	HMBC	ROESY
Xyl1 (1→C-3)				
1	104.7 CH	4.73 d (8.5)	C: 3	H-3; H-3, 5 Xyl1
2	79.7 CH	4.18 t (8.5)	C: 1 Glc2; C: 1 Xyl1	H-4 Xyl1; H-1 Glc2
3	75.5 CH	4.34 t (9.2)	C: 4 Xyl1	H-1 Xyl1
4	76.1 CH	4.99 m		
5	64.2 CH ₂	4.78 dd (5.0; 11.4) 3.79 dd (8.5; 11.4)	C: 4 Xyl1	
Glc2 (1→2Xyl1)				
1	101.4 CH	5.39 d (6.8)	C: 2 Xyl1	H-2 Xyl1; H-5 Glc2
2	82.2 CH	3.96 t (8.9)	C: 1 Xyl5, C: 1, 3 Glc2	H-1 Xyl5
3	75.5 CH	4.08 t (8.9)	C: 2, 4 Glc2	H-1 Glc2
4	80.6 CH	4.01 t (8.9)	C: 1 Glc3; C: 5 Glc2	H-1 Glc3
5	75.8 CH	3.68 m		H-1 Glc2
6	61.4 CH ₂	4.34 brd (11.6) 4.25 dd (5.5; 11.6)		
Glc3 (1→4Glc2)				
1	103.6 CH	4.96 d (8.0)	C: 4 Glc2	H-4 Glc2; H-3, 5 Glc3
2	73.5 CH	3.91 t (8.6)	C: 1, 3 Glc3	
3	86.7 CH	4.16 t (8.6)	C: 2, 4 Glc3	H-1 MeGlc4
4	69.2 CH	3.87 m		
5	77.0 CH	3.85 m		H-1 Glc3
6	61.1 CH ₂	4.24 brd (9.6) 3.99 dd (4.8; 11.8)		
MeGlc4 (1→3Glc3)				
1	104.5 CH	5.16 d (7.6)	C: 3 Glc3	H-3 Glc3; H-3, 5 MeGlc4
2	74.5 CH	3.85 t (8.3)	C: 1, 3 MeGlc4	
3	86.9 CH	3.67 t (8.3)	OMe	H-1 MeGlc4; OMe
4	70.1 CH	3.89 t (8.3)	C: 5 MeGlc4	
5	77.5 CH	3.91 m		H-1 MeGlc4
6	61.7 CH ₂	4.35 brd (11.9)	C: 4 MeGlc4	

Table 4. Cont.

Atom	δ_C mult. ^a	δ_H mult. (<i>J</i> in Hz) ^{b,c,d}	HMBC	ROESY
OMe	60.7 CH ₃	4.03 dd (5.9; 11.9) 3.81 s	C: 4, 5 MeGlc4 C: 3 MeGlc4	
Xyl15 (1→2Glc2)				
1	105.2 CH	5.19 d (7.1)	C: 2 Glc2	H-2 Glc2; H-3, 5 Xyl15
2	74.7 CH	3.94 t (8.3)	C: 1, 3 Xyl15	
3	76.3 CH	4.04 t (8.3)	C: 2 Xyl15	H-1 Xyl15
4	70.3 CH	4.09 dd (5.1; 9.0)		
5	66.3 CH ₂	4.31 dd (5.1; 11.5) 3.59 t (10.3)		H-1 Xyl15

^a Recorded at 125.67 MHz in C₅D₅N/D₂O. ^b Recorded at 500.12 MHz in C₅D₅N/D₂O. ^c Bold—interglycosidic positions. ^d Italics—sulfate positions. Multiplicity by 1D TOCSY. The original spectra of **2** are provided in Figures S9–S15.

The fragment ion peaks in the (–)ESI-MS/MS of **2** (Figure S16) were observed at *m/z* 1296.5 [M_{Na} – Na – CH₃COOH][–], 1105.5 [M_{Na} – Na – SO₃Na – Xyl + H][–], 843.2 [M_{Na} – Na – Agl – H][–], and 723.3 [M_{Na} – Na – Agl – NaSO₄][–] due to fragmentation of the [M_{Na} – Na][–] ion with *m/z* 1355.6. The ion peak at *m/z* 589.2 [M_{Na} – Na – MeGlc]^{2–} appeared as a result of the fragmentation of the [M_{Na} – Na – H]^{2–} ion at *m/z* 677.3. The (+)ESI-MS/MS of **2** demonstrated the fragmentation of the [M_{Na} + Na]⁺ ion with *m/z* 1401.5, giving ion peaks at *m/z* 1281.6 [M_{Na} + Na – NaHSO₄]⁺ and 1209.6 [M_{Na} + Na – MeGlc + H]⁺.

Thus, djakonovioside D₁ (**2**) is 3β-*O*-[3-*O*-methyl-β-*D*-glucopyranosyl-(1→3)-β-*D*-glucopyranosyl-(1→4)-[(1→2)-β-*D*-xylopyranosyl]-β-*D*-glucopyranosyl-(1→2)-4-*O*-sodium sulfate-β-*D*-xylopyranosyl]-16β-acetoxylolosta-7,24-dien.

The molecular formula of djakonovioside E₁ (**3**) was determined as C₅₆H₈₅O₃₃S₃Na₃ from the [M_{3Na} – Na][–] ion peak at *m/z* 1427.3942 (calc. 1427.3936), the [M_{3Na} – 2Na]^{2–} ion peak at *m/z* 702.2037 (calc. 702.2022), and the three-charged ion [M_{3Na} – 3Na]^{3–} at *m/z* 460.4732 (calc. 460.4717) in the (–)HR-ESI-MS (Figure S24) that confirmed the presence of three sulfate groups. In the ¹H and the ¹³C NMR spectra of the carbohydrate chain of djakonovioside E₁ (**3**) (Table 5, Figures S17–S23), the four doublets of the anomeric protons at δ_H 4.68–5.09 (*J* = 7.3–8.5 Hz) and the signals of the corresponding anomeric carbons at δ_C 103.8–104.7 were indicative of a tetrasaccharide chain with β-glycosidic bonds between sugars. The first monosaccharide connected to the C-3 of the aglycone was a xylose (Xyl1) sulfated by C-4 (deduced from the deshielding of this signal to δ_C 76.1). The subsequent analysis of the 1D TOCSY, ¹H,¹H COSY, HSQC, and ROESY spectra revealed that the second residue was a glucose, which was linked to C-2 Xyl1. The third sugar—glucose (Glc3)—was attached to the typical position—C-4 Glc2 (cross-peak H-1 Glc3/H-4 Glc2 in the ROESY spectrum)—and was sulphated by C-6 (deshielding of the signal of C-6 Glc3 to δ_C 67.4). Terminal 3-*O*-methylglucose residue was bound to C-3 Glc3, that was deduced from the corresponding NOE correlation (Table 5) and also contained a sulphate group because the signal of C-6 MeGlc4 was observed at δ_C 67.0. Hence, the tetrasaccharide chain of **3** was new, having glucose as the second unit and bearing three sulfate groups.

The fragment ion peaks in the (–)ESI-MS/MS of **3** (Figure S24) were observed as a result of the fragmentation of the [M_{3Na} – Na][–] ion at *m/z* 1427.5, giving ions at *m/z* 1367.4 [M_{3Na} – Na – CH₃COOH][–], 1307.4 [M_{3Na} – Na – NaHSO₄][–], 1029.4 [M_{3Na} – Na – NaHSO₄–MeGlcSO₃ + H][–], 915.1 [M_{3Na} – Na – Agl – H][–], 681.1 [M_{3Na} – Na – Agl – XylSO₃ – H][–], and 519.0 [M_{3Na} – Na – Agl – XylSO₃ – Glc – H][–]. The ion peak at *m/z* 446.0 [M_{3Na} – 2Na – Agl – H]^{2–} appeared as a result of the fragmentation of the [M_{3Na} – 2Na]^{2–} ion at *m/z* 704.2.

Thus, djakonovioside E₁ (**3**) is 3β-*O*-[6-*O*-sodium sulfate-3-*O*-methyl-β-*D*-glucopyranosyl-(1→3)-6-*O*-sodium sulfate-β-*D*-glucopyranosyl-(1→4)-β-*D*-glucopyranosyl-(1→2)-4-*O*-sodium sulfate-β-*D*-xylopyranosyl]-16β-acetoxylolosta-7,25-dien.

The molecular formula of djakonovioside F₁ (**4**) was determined as C₅₉H₉₃O₃₄S₃Na₃ from the [M_{3Na} – Na][–] ion peak at *m/z* 1487.4467 (calc. 1487.4511), the [M_{3Na} – 2Na]^{2–} ion peak at *m/z* 732.2320 (calc. 732.2310), and the [M_{3Na} – 3Na]^{3–} ion peak at *m/z* 480.4926 (calc. 480.4909) in the (–)HR-ESI-MS (Figure S32). Noticeably, for the isotope composition of the pseudomolecular ion of **4**, the predominance of the [M_{3Na} – Na + 2][–] ion peak is inherent. A normal isotope distribution was observed for two- and three-charged pseudomolecular ions. This is obviously explained by the chemical structure of the side chain. The protons of the methylene group CH₂-23 adjacent to the 22-oxo group and the 24(25)-double bond were easily exchanged to deuterium when the glycoside was dissolved in the mixture C₅D₅N/D₂O for the NMR spectra acquisition. The signal of CH₂-23 could not be accumulated in the ¹³C NMR spectrum of **4** for the same reason. Therefore, the spectra were repeatedly acquired in C₅D₅N/H₂O, which resulted in the appearance of the signal at δ_C 37.0 that corresponded to the proton's signal at δ_H 3.61 (m, H-23) in the HSQC spectrum.

The aglycone of djakonovioside F₁ (**4**) (Table 6; Figures S25–S30) did not contain a γ-lactone ring (deduced from the absence of the characteristic signal in the ¹³C NMR spectrum at δ_C ~180 (C-18)) being of the non-holostane type. Actually, the signals of CH₃-18 were observed at δ_C 24.5 and δ_H 1.29 (s). The signals in the downfield region of the ¹³C and ¹H NMR spectra at δ_C 122.1 (C-7), δ_H 5.61 (m, H-7), and 148.5 (C-8) were characteristic of the intranuclear double bond, while the signals at δ_C 117.3 (C-24), δ_H 5.46 (m, H-24), and δ_C 134.9 (C-25) indicated the availability of a normal side chain with the 24(25)-double bond in **4**. The signals of the side chain were deduced starting from the signal for C-22. The signal of C-22 was assigned on the basis of HMBC correlations of H-21/C: 20, 22 those are typical for lanostane derivatives. Hence, the signal of quaternary carbon C-22 was observed at δ_C 216.1, indicating the presence of an oxo-group. The position of the double bond was assigned as 24(25) based on the HMBC correlations of H-26(27)/C: 24, 25. The (20*R*)-configuration, the same as in lanostane derivatives from sea cucumbers having an oxygen-containing substituent at C-22 [17], was determined on the basis of NOE-correlations H-21/H-12 and H-21/H-17.

Table 5. ¹³C and ¹H NMR chemical shifts and HMBC and ROESY correlations of carbohydrate moiety of djakonovioside E₁ (**3**).

Atom	δ _C mult. ^a	δ _H mult. (J in Hz) ^{b,c,d}	HMBC	ROESY
Xyl1 (1→C-3)				
1	104.7 CH	4.68 d (7.3)	C: 3; C: 5 Xyl1	H-3; H-3, 5 Xyl1
2	81.2 CH	4.07 dd (9.0; 7.3)	C: 1 Glc2; C: 3 Xyl1	
3	74.6 CH	4.25 t (9.0)	C: 2, 4 Xyl1	H-1 Xyl1
4	76.0 CH	4.94 ddd (14.3; 9.0; 6.4)	C: 3 Xyl1	
5	63.8 CH ₂	4.74 dd (12.2; 5.3)	C: 3 Xyl1	
		3.72 dd (12.2; 10.1)	C: 1 Xyl1	H-1, 3 Xyl1
Glc2 (1→2Xyl1)				
1	104.3 CH	5.07 d (8.0)	C: 2 Xyl1; C: 2 Glc2	H-2 Xyl1; H-3, 5 Glc2
2	75.1 CH	3.85 t (8.7)	C: 3 Glc2	
3	75.2 CH	3.97 t (8.7)	C: 4 Glc2	H-1 Glc2
4	81.8 CH	3.95 t (8.7)	C: 1 Glc3; C: 3 Glc2	H-1 Glc3
5	75.9 CH	3.68 t (8.7)	C: 4 Glc2	H-1 Glc2
6	61.1 CH ₂	4.26 m		
Glc3 (1→4Glc2)				
1	103.8 CH	4.87 d (8.5)	C: 4 Glc2	H-4 Glc2; H-3, 5 Glc3
2	73.4 CH	3.81 t (8.7)	C: 1, 3 Glc3	
3	86.4 CH	4.07 t (8.7)	C: 1 MeGlc4; C: 2, 4 Glc3	H-1 MeGlc4; H-1 Glc3
4	69.4 CH	3.74 t (8.7)	C: 5, 6 Glc3	
5	74.8 CH	4.03 m		
6	67.4 CH ₂	4.93 brd (10.9)		
		4.55 dd (10.9; 6.5)	C: 5 Glc3	

Table 5. Cont.

Atom	δ_C mult. ^a	δ_H mult. (J in Hz) ^{b,c,d}	HMBC	ROESY
MeGlc4 (1→3Glc3)				
1	104.7 CH	5.09 d (7.9)	C: 3 Glc3; C: 2 MeGlc4	H-3 Glc3; H-3, 5 MeGlc4
2	74.3 CH	3.76 t (8.5)	C: 1 MeGlc4	
3	86.4 CH	3.61 t (8.5)	OMe; C: 2, 4 MeGlc4	H-1, 5 MeGlc4
4	69.8 CH	3.96 m	C: 3, 5, 6 MeGlc4	
5	75.4 CH	4.00 m	C: 4 MeGlc4	H-1 MeGlc4
6	67.0 CH ₂	4.91 brd (11.2)	C: 4 MeGlc4	
		4.70 brd (9.3)	C: 4, 5 MeGlc4	
OMe	60.5 CH ₃	3.75 s	C: 3 MeGlc4	

^a Recorded at 125.67 MHz in C₅D₅N/D₂O. ^b Recorded at 500.12 MHz in C₅D₅N/D₂O. ^c Bold—interglycosidic positions. ^d Italics—sulfate positions. Multiplicity by 1D TOCSY. The original spectra of **3** are provided in Figures S17–S23.

The ¹H and ¹³C NMR spectra of the carbohydrate part of djakonovioside F₁ (**4**) (Table 7; Figures S25–S31) were characteristic for the pentasaccharide chain (five doublets of anomeric protons at δ_H 4.71–5.20 and corresponding to the signals of the anomeric carbons at δ_C 102.1–105.2) with β -glycosidic bonds (coupling constants of anomeric protons $J = 7.2$ – 8.1 Hz). The monosaccharide composition deduced from the analysis of the 1D TOCSY, ¹H,¹H COSY, HSQC, and ROESY spectra was two xylose (Xyl1 and Xyl5), quinovose (Qui2), glucose (Glc3), and 3-*O*-methylglucose (MeGlc4) residues. Analysis of the ROESY and HMBC spectra of **4** revealed that the quinovose was a branchpoint of the chain because Xyl5 attached to C-2 Qui2. The rest of the glycosidic bonds occupied typical positions for the glycosides of the sea cucumbers, demonstrating the glycosylation effects in the NMR spectra: $\delta_{C-2\text{Xyl1}}$ 81.5, $\delta_{C-4\text{Qui2}}$ 86.4, and $\delta_{C-3\text{Glc3}}$ 86.6. Three sulphate groups were present in the sugar chain of **4** in the following positions, which were deduced on the basis of α -shifting effects: C-4 Xyl1 (δ_C 76.1), C-6Glc3 (δ_C 67.3), and C-6 MeGlc4 (δ_C 66.4). The same carbohydrate chain composed the molecules of isokoreoside A (**9**) (Table S7; Figures S52–S57) and koreoside A (**10**) (Table S9).

Table 6. ¹³C and ¹H NMR chemical shifts and HMBC and ROESY correlations of aglycone moiety of djakonovioside F₁ (**4**).

Position	δ_C mult. ^a	δ_H mult. (J in Hz) ^b	HMBC	ROESY
1	35.6 CH ₂	1.30 m		H-3, H-5
2	26.9 CH ₂	1.94 m		H-31,
		1.77 m		H-19, H-30
3	88.8 CH	3.14 dd (3.8; 11.4)	C: 30, 31, C: 1 Xyl1	H-1, H-5, H-31, H1-Xyl1
4	39.4 C			
5	49.6 CH	0.85 dd (3.2; 11.4)	C: 4, 10, 19, 30	H-1, H-3, H-31
6	23.1 CH ₂	1.93 m		H-19
		1.85 m		
7	122.1 CH	5.61 m	C: 9, 13	H-15, H-32
8	148.5 C			
9	48.1 CH	2.29 brd (13.3)		H-18, H-19
10	35.5 C			
11	22.8 CH ₂	1.66 m		
		1.42 m		
12	34.9 CH ₂	1.97 m		H-17, H-21
		1.76 m		
13	52.8 C			
14	45.1 C			
15	33.4 CH ₂	1.64 m		H-18

Table 6. Cont.

Position	δ_C mult. ^a	δ_H mult. (J in Hz) ^b	HMBC	ROESY
16	22.3 CH ₂	1.56 m 2.02 m 1.56 m	C: 14, 32	H-7 H-18 H-21, H-32
17	53.2 CH	2.38 t (8.9)	C: 14, 16, 18, 21	H-12, H-21, H-32
18	24.5 CH ₃	1.29 s	C: 12, 13, 14	H-9, H-12, H-15, H-16, H-19
19	24.6 CH ₃	0.93 s	C: 1, 5, 9, 10	H-2, H-6, H-9, H-18, H-30
20	81.4 C			
21	24.9 CH ₃	1.60 s	C: 17, 20, 22	H-12, H-17, H-18
22	216.1 C			
23	37.0 CH ₂ *	3.61 m		
24	117.3 CH	5.46 m	C: 26, 27	H-26
25	134.9 C			
26	25.5 CH ₃	1.63 s	C: 24, 25, 27	H-24
27	17.9 CH ₃	1.56 s	C: 24, 25, 26	
30	17.5 CH ₃	1.03 s	C: 3, 4, 5, 31	H-2, H-6, H-19, H-31
31	28.7 CH ₃	1.18 s	C: 3, 4, 5, 30	H-3, H-5, H-6, H-30, H-1 Xyl1
32	30.7 CH ₃	1.07 s	C: 8, 13, 14, 15	H-7, H-12, H-15, H-17

^a Recorded at 125.67 MHz in C₅D₅N/D₂O. ^b Recorded at 500.12 MHz in C₅D₅N/D₂O. * Recorded at 176.04 MHz in C₅D₅N/H₂O. The original spectra of **4** are provided in Figures S25–S30.

The fragment ion peaks in the (–)ESI-MS/MS of **4** (Figure S32) were observed as a result of the fragmentation of the [M₃Na – Na + 2][–] isotopic ion at *m/z* 1489.5, giving the ions at *m/z* 1211.4 [M₃Na – Na + 2 – MeGlcSO₃][–], 947.4 [M₃Na – Na + 2 – MeGlcSO₃ – GlcSO₃][–], and 797.1 [M₃Na – Na + 2 – MeGlcSO₃ – GlcSO₃ – XylSO₃ – H][–], arising as a result of the sequential loss of monosaccharide units.

Thus, djakonovioside F₁ (**4**) is 3β-*O*-{6-*O*-sodium sulfate-3-*O*-methyl-β-*D*-glucopyranosyl-(1→3)-6-*O*-sodium sulfate-β-*D*-glucopyranosyl-(1→4)-[(1→2)-β-*D*-xylopyranosyl]-β-*D*-quinovopyranosyl-(1→2)-4-*O*-sodium sulfate-β-*D*-xylopyranosyl}-(2*OR*)-hydroxy-22-oxo-lanosta-7,24-dien.

Table 7. ¹³C and ¹H NMR chemical shifts and HMBC and ROESY correlations of carbohydrate moiety of djakonovioside F₁ (**4**).

Atom	δ_C mult. ^a	δ_H mult. (J in Hz) ^{b,c,d}	HMBC	ROESY
Xyl1 (1→C-3)				
1	104.6 CH	4.71 d (7.4)	C: 3	H-3; H-3, 5 Xyl1
2	81.5 CH	3.97 dd (9.1; 7.4)	C: 1 Qui2; C: 1, 3 Xyl1	H-1 Qui2; H-4 Xyl1
3	75.2 CH	4.30 t (9.1)	C: 2, 4 Xyl1	H-1, 5 Xyl1
4	76.1 CH	5.00 ddd (13.8; 9.1; 5.6)	C: 3 Xyl1	H-2 Xyl1
5	64.1 CH ₂	4.79 dd (12.6; 5.6)	C: 1, 3 Xyl1	
		3.86 t (10.8)	C: 1, 4 Xyl1	H-1, 3 Xyl1
Qui2 (1→2Xyl1)				
1	102.1 CH	5.18 d (7.2)	C: 2 Xyl1	H-2 Xyl1; H-5 Qui2
2	82.45CH	3.91 t (8.6)	C: 1, 3 Qui2; C: 1 Xyl5	H-1 Xyl5; H-4 Qui2
3	75.2 CH	3.97 t (8.6)	C: 2, 4 Qui2	H-1, 5 Qui2
4	86.4 CH	3.43 t (8.6)	C: 1 Glc3; C: 3, 5 Qui2	H-1 Glc3; H-2, 6 Qui2
5	70.8 CH	3.56 dd (8.6; 5.9)	C: 4 Qui2	H-1, 3 Qui2
6	17.9 CH ₃	1.56 d (5.9)	C: 5, 6 Qui2	H-4 Qui2
Glc3 (1→4Qui2)				
1	103.9 CH	4.76 d (8.1)	C: 4 Qui2	H-4 Qui2; H-3, 5 Glc3
2	73.4 CH	3.80 t (8.8)	C: 1, 3 Glc3	
3	86.6 CH	4.10 t (8.8)	C: 1 MeGlc4; C: 2, 4 Glc3	H-1 MeGlc4; H-1 Glc3
4	69.1 CH	3.80 m	C: 3, 5, 6 Glc3	
5	74.9 CH	4.06 m		
6	67.3 CH ₂	4.94 brd (10.8)		

Table 7. Cont.

Atom	δ_C mult. ^a	δ_H mult. (J in Hz) ^{b,c,d}	HMBC	ROESY
		4.58 dd (10.8; 5.4)	C: 5 Glc3	
MeGlc4 (1→3Glc3)				
1	104.8 CH	5.13 d (8.1)	C: 3 Glc3; C: 2 MeGlc4	H-3 Glc3; H-3, 5 MeGlc4
2	74.4 CH	3.76 t (8.8)	C: 1 MeGlc4	H-4 MeGlc4
3	86.4 CH	3.62 t (8.8)	OMe; C: 4 MeGlc4	H-1 MeGlc4
4	69.8 CH	3.99 m	C: 5 MeGlc4	
5	75.6 CH	3.99 m		H-1, 3 MeGlc4
6	67.0 CH ₂	4.93 d (11.4)	C: 4, 5 MeGlc4	
		4.75 brd (11.4)	C: 5 MeGlc4	
OMe	60.5 CH ₃	3.75 s	C: 3 MeGlc4	
Xyl5 (1→2Qui2)				
1	105.2 CH	5.20 d (7.4)	C: 2 Qui2	H-2 Qui2; H-3,5 Xyl5
2	74.9 CH	3.92 t (8.1)	C: 3 Xyl5	
3	76.3 CH	4.07 t (8.1)	C: 2, 4 Xyl5	H-1 Xyl5
4	70.1 CH	4.04 m		
5	66.4 CH ₂	4.27 dd (11.8; 5.2)	C: 1, 3, 4 Xyl5	H-1, 3 Xyl5
		3.63 t (10.3)		

^a Recorded at 125.67 MHz in C₅D₅N/D₂O. ^b Recorded at 500.12 MHz in C₅D₅N/D₂O. ^c Bold—interglycosidic positions. ^d Italics—sulfate positions. Multiplicity by 1D TOCSY. The original spectra of **4** are provided in Figures S25–S31.

The structures of known compounds, okhotoside A₂-1 (**5**) from *C. okhotensis* [18], cucumarioside A₂-5 (**6**) from *C. conicospermium* [19], frondoside A₂-3 (**7**) from *C. frondosa* [20], and koreoside A (**10**) from *C. koreaensis* [21], were identified by extensive analysis of the 1D and 2D NMR spectra and compared with the literature data. All the original spectra and the assignments of the signals are provided in Tables S2–S9 and Figures S33–S57.

Isokoreoside A (**9**) (Tables S7–S8; Figures S52–S57) was first isolated as a desulfated derivative from the fraction of the trisulfated glycosides of *C. conicospermium* [19], which was separated into individual compounds after the procedure of solvolytic desulfation. In native form, this compound was later obtained from *C. frondosa* [17].

Cucumarioside A₃-2 (**8**) was isolated as native glycoside from *C. djakonovi* for the first time. The structure of **8** was determined earlier on the basis of its desulfated derivative, obtained the same way as **9** from *Cucumaria conicospermium* [19]. So, the 2D NMR spectra and the assignments of the signals of **8** are provided first (Tables 8 and 9, Figures S45–S51).

Table 8. ¹³C and ¹H NMR chemical shifts and HMBC and ROESY correlations of aglycone moiety of cucumarioside A₃-2 (**8**).

Position	δ_C mult. ^a	δ_H mult. (J in Hz) ^b	HMBC	ROESY
1	35.5 CH ₂	1.29 m		H-3, H-11, H-19
2	26.8 CH ₂	1.93 m		H-31
		1.74 m		H-19, H-30
3	88.8 CH	3.15 dd (4.1; 11.6)	C: 4, 30, 31, C: 1 Xyl1	H-1, H-5, H-31, H1-Xyl1
4	39.4 C			
5	48.7 CH	0.85 dd (3.3; 11.6)	C: 4, 6, 10, 19, 30	H-3, H-31
6	23.1 CH ₂	1.90 m		
		1.81 m		H-19, H-30
7	122.5 CH	5.58 m	C: 9, 14	H-15
8	147.6 C			
9	48.1 CH	2.13 m	C: 11	H-18, H-19
10	35.5 C			
11	22.3 CH ₂	1.68 m		H-1, H-18
		1.40 m		H-32

Table 8. Cont.

Position	δ_C mult. ^a	δ_H mult. (J in Hz) ^b	HMBC	ROESY
12	33.3 CH ₂	2.00 m 1.67 m		H-17 H-18
13	44.9 C			
14	53.1 C			
15	33.3 CH ₂	1.68 m 1.52 m		H-7, H-18
16	22.4 CH ₂	2.28 m		
17	61.9 CH	2.75 t (8.7)	C: 13, 18, 20	H-12, H-15, H-21, H-32
18	24.7 CH ₃	0.78 s	C: 12, 13, 14, 17	H-9, H-12, H-15, H-16
19	24.3 CH ₃	0.91 s	C: 1, 9, 10	H-1, H-2, H-6, H-9, H-30
20	211.6 C			
21	30.6 CH ₃	2.16 s	C: 17, 20	H-12, H-17
30	17.3 CH ₃	1.02 s	C: 3, 4, 5, 31	H-2, H-6, H-19, H-31
31	28.7 CH ₃	1.18 s	C: 3, 4, 5, 30	H-3, H-5, H-6, H-30, H-1 Xyl1
32	30.4 CH ₃	1.04 s	C: 8, 13, 14, 15	H-7, H-11, H-12, H-15, H-17

^a Recorded at 125.67 MHz in C₅D₅N/D₂O. ^b Recorded at 500.12 MHz in C₅D₅N/D₂O. The original spectra of **8** are provided in Figures S45–S51.

Table 9. ¹³C and ¹H NMR chemical shifts and HMBC and ROESY correlations of carbohydrate moiety of cucumarioside A₃-2 (**8**).

Atom	δ_C mult. ^a	δ_H mult. (J in Hz) ^{b,c,d}	HMBC	ROESY
Xyl1 (1→C-3)				
1	104.5 CH	4.72 d (7.0)	C: 3; C: 5 Xyl1	H-3; H-3, 5 Xyl1
2	81.4 CH	3.96 t (8.3)	C: 1 Qui2; C: 1, 3 Xyl1	H-4 Xyl1; H-1 Qui2
3	75.0 CH	4.31 t (8.3)	C: 2, 4 Xyl1	
4	76.1 CH	5.00 m	C: 3 Xyl1	H-2 Xyl1
5	64.1 CH ₂	4.79 dd (5.1; 11.5) 3.87 dd (8.5; 11.5)	C: 1, 3 Xyl1	
Qui2 (1→2Xyl1)				
1	102.1 CH	5.18 d (8.4)	C: 2 Xyl1	H-2 Xyl1; H-3, 5 Qui2
2	82.3 CH	3.93 t (9.0)	C: 1 Xyl5; C: 1, 3 Qui2	H-1 Xyl5
3	75.3 CH	3.99 t (9.0)	C: 2, 4 Qui2	
4	86.4 CH	3.46 t (9.0)	C: 1 Glc3; C: 3, 5 Qui2	H-1 Glc3; H-2 Qui2
5	70.8 CH	3.57 dd (6.4; 9.0)	C: 4 Qui2	H-1 Qui2
6	17.8 CH ₃	1.57 d (6.4)		
Glc3 (1→4Qui2)				
1	104.0 CH	4.78 d (7.5)	C: 4 Qui2	H-4 Qui2; H-3, 5 Glc3
2	73.5 CH	3.83 t (8.9)	C: 1, 3 Glc3	
3	85.9 CH	4.18 t (8.9)	C: 1 MeGlc4; C: 2, 4 Glc3	H-1 MeGlc4; H-1, 5 Glc3
4	69.0 CH	3.87 t (8.9)	C: 3, 5, 6 Glc3	
5	75.2 CH	4.05 m		H-1 Glc3
6	67.1 CH ₂	4.94 d (10.3) 4.62 dd (6.2; 10.3)	C: 5 Glc3	
MeGlc4 (1→3Glc3)				
1	104.4 CH	5.21 d (8.2)	C: 3 Glc3	H-3 Glc3; H-5 MeGlc4
2	74.5 CH	3.85 t (8.2)	C: 1, 3 MeGlc4	
3	87.0 CH	3.67 t (8.2)	OMe; C: 2, 4 MeGlc4	H-1 MeGlc4; OMe
4	70.3 CH	3.89 m	C: 5 MeGlc4	
5	77.5 CH	3.89 m	C: 4 MeGlc4	H-1 MeGlc4
6	61.7 CH ₂	4.34 d (11.7) 4.05 brd (11.7) 3.80 s	C: 4, 5 MeGlc4 C: 3 MeGlc4	
OMe	60.6 CH ₃			
Xyl5 (1→2Qui2)				
1	105.1 CH	5.22 d (7.5)	C: 2 Qui2	H-2 Qui2; H-3, 5 Xyl5
2	74.9 CH	3.92 t (7.5)	C: 1 Xyl5	

Table 9. Cont.

Atom	δ_C mult. ^a	δ_H mult. (J in Hz) ^{b,c,d}	HMBC	ROESY
3	76.4 CH	4.06 t (7.5)	C: 2, 4 Xyl5	
4	70.1 CH	4.04 m		
5	66.4 CH ₂	4.28 dd (4.8; 11.7) 3.65 brdd (9.0; 11.7)	C: 1, 3, 4 Xyl5 C: 3, 4 Xyl5	H-1 Xyl5

^a Recorded at 125.67 MHz in C₅D₅N/D₂O. ^b Recorded at 500.12 MHz in C₅D₅N/D₂O. ^c Bold—interglycosidic positions. ^d Italics—sulfate positions. Multiplicity by 1D TOCSY. The original spectra of **8** are provided in Figures S45–S51.

2.2. Biologic Activity of the Glycosides

The cytotoxic activity of the compounds isolated from *C. djakonovi* was studied against three types of human breast cancer cells (MCF-7, T-47D, and triple negative MDA-MB-231), as well as the non-tumor mammary epithelial cell line MCF-10A. Djakonovioside A₁ [5] and cisplatin were used as the positive controls. Cytotoxic activity against all the selected cell lines was assessed using the MTT method (Table 10).

Table 10. The cytotoxic activities of glycosides **1–10**, djakonovioside A₁, and cisplatin (positive controls) against human erythrocytes and MCF-10A, MCF-7, T-47D, and MDA-MB-231 human cell lines.

Glycosides	ED ₅₀ , μ M, Erythrocytes	Cytotoxicity, IC ₅₀ μ M			
		MCF-10A	MCF-7	T-47D	MDA-MB-231
djakonovioside C ₁ (1)	8.55 ± 0.04	21.79 ± 0.72	38.64 ± 2.36	16.82 ± 0.76	7.67 ± 0.32
djakonovioside D ₁ (2)	7.74 ± 0.37	>50.0	>50.0	>50.0	>50.0
djakonovioside E ₁ (3)	21.67 ± 0.94	>50.0	1.52 ± 0.14	>50.0	2.19 ± 0.17
djakonovioside F ₁ (4)	0.51 ± 0.01	23.21 ± 0.78	36.75 ± 0.73	22.53 ± 1.78	20.04 ± 0.63
okhotoside A ₂ -1 (5)	1.53 ± 0.14	12.16 ± 0.16	39.81 ± 0.18	11.86 ± 0.42	12.6 ± 0.16
cucumarioside A ₂ -5 (6)	1.63 ± 0.13	14.02 ± 1.03	25.68 ± 1.49	5.81 ± 0.86	2.58 ± 0.10
frondoside A ₂ -3 (7)	>50.0	>50.0	>50.0	>50.0	>50.0
cucumarioside A ₃ -2 (8)	17.91 ± 0.48	>50.0	>50.0	>50.0	>50.0
isokoreoside A (9)	17.44 ± 0.57	>50.0	>50.0	>50.0	>50.0
koreoside A (10)	>50.0	>50.0	>50.0	>50.0	>50.0
djakonovioside A ₁	2.52 ± 0.23	17.51 ± 0.54	26.43 ± 0.14	15.25 ± 0.96	12.05 ± 0.54
cisplatin	-	77.31 ± 1.32	109.42 ± 2.01	>160.0	76.60 ± 1.20

Djakonovioside F₁ (**4**), okhotoside A₂-1 (**5**), and cucumarioside A₂-5 (**6**) showed strong hemolytic activity against human erythrocytes, with ED₅₀ 0.51 ± 0.01, 1.53 ± 0.14, and 1.63 ± 0.13 μ M, respectively. The hemolytic activity of djakonoviosides C₁ (**1**) and D₁ (**2**) was slightly lower but significant and close to each other. Djakonovioside D₁ (**2**), cucumarioside A₃-2 (**8**), and isokoreoside A (**9**) demonstrated moderate hemolytic activity but were not active against all human tumor cell lines. Frondoside A₂-3 (**7**) and koreoside A (**10**) did not show hemolytic or cytotoxic activity in the concentration range up to 50 μ M.

The estimation of the selectivity index (Table 11) showed djakonovioside E₁ (**3**) was a leader, demonstrating the strongest cytotoxicity against the MCF-7 cell line (IC₅₀ 1.52 ± 0.14 μ M) as well as against the triple negative MDA-MB-231 cell line (IC₅₀ 2.19 ± 0.17 μ M). At the same time, this glycoside was not toxic in relation to normal mammary epithelial cells (MCF-10A). None of the other glycosides showed similar selectivity. But the MDA-MB-231 cell line was more sensitive to their action compared with the T-47D and, especially, MCF-7 cell lines.

Table 11. Tumor cell selectivity index (SI; a ratio of IC₅₀ calculated for healthy and cancer cells) of tested glycosides.

No.	Glycoside	Selectivity Index (SI)		
		MCF-7	T-47D	MDA-MB-231
1	djakonovioside C ₁	0.56	1.34	2.84
3	djakonovioside E ₁	>32.89	-	>22.83
5	okhotoside A ₂ -1	0.31	1.03	0.97
4	djakonovioside F ₁	0.63	1.02	1.16
6	cucumarioside A ₂ -5	0.55	2.41	5.43
	djakonovioside A ₁	0.66	1.15	1.45
	cisplatin	0.71	<0.48	1.01

The cytotoxic activity of djakonovioside E₁ (3) was maximal in the series against the MCF-7 and MDA-MB-231 cell lines with a half-maximal inhibitory concentration of $1.52 \pm 0.14 \mu\text{M}$ (Figure 2a) and $2.19 \pm 0.17 \mu\text{M}$ (Table 10), respectively. Cucumarioside A₂-5 (6) was the most active compound from the series in relation to T-47D cells (IC₅₀ $5.81 \pm 0.86 \mu\text{M}$ (Figure 2b). Djakonovioside C₁ (1) and cucumarioside A₂-5 (6) demonstrated a pronounced effects against the MDA-MB-231 cell line (IC₅₀ of 7.67 ± 0.32 and $2.58 \pm 0.1 \mu\text{M}$, respectively) (Figure 2c,d).

To study antiproliferative properties, three most active glycosides were selected: djakonoviosides C₁ (1) and E₁ (3) and cucumarioside A₂-5 (6). The prolonged incubation of cells for 48 and 72 h with glycosides 1 and 6 did not increase their EC₅₀; but, more importantly, the glycosides did not lose cytotoxicity over time. Only djakonovioside E₁ (3) showed an antiproliferative effect when incubated with MCF-7 cells for 48 h, demonstrating approximately a two-fold increase in EC₅₀ ($0.78 \pm 0.32 \mu\text{M}$) (Figure 2a).

The clonogenic (or colony formation) assay is a standard in vitro cell survival assay based on the ability of a single cell to grow into a colony. In the human body, this uncontrolled growth of tumor cells leads to the formation of metastases. To study the effect of selected glycosides on the formation and growth of tumor cell colonies, a range of non-toxic concentrations was used against the MDA-MB-231 cell line (Figure 3a). Additionally, colonies of MCF-7 lines were exposed to the action of non-toxic doses of djakonovioside E₁ (3) (Figure 3b). For all tested compounds, a dose-dependent effect of inhibiting colony growth was observed. Cucumarioside A₂-5 (6) at a concentration of 1 μM demonstrated the greatest inhibitory effect on the formation and growth of colonies: $44.32 \pm 0.77\%$ of the control. The inhibitory effects of djakonovioside C₁ (1) at concentrations of 2 and 1 μM were the same—approximately 25% compared to the control. Djakonovioside E₁ (3) blocked the formation of colonies of both MDA-MB-231 and MCF-7 to the same extent: at a concentration of 2 μM in relation to MDA-MB-231 cells to $35.68 \pm 2.00\%$ of the control and in relation to MCF-7 cells to $30.73 \pm 0.49\%$ of the control (Figure 3a,b).

Scratch analysis is used to study the effects of compounds with potential antitumor activity on cell motility and cell–cell interactions. In the control group of the MDA-MB-231 cell line, the scratch was overgrown within 24 h, while in the control group of the MCF-7 cell line, this happened after 72 h (Figure 4e). All the selected glycosides in the concentration range below their EC₅₀ inhibited the migration of breast cancer MDA-MB-231 and MCF-7 cells in a dose-dependent manner. The greatest effect, about 85% as compared to the control, was observed for cucumarioside A₂-5 (6) at a concentration of 1 μM after 24 h of incubation with MDA-MB-231 cells (Figure 4b). Images of CFDA SE fluorescently labeled MCF-7 cells incubated with djakonovioside E₁ (3) demonstrate the reliable blockage of the migration of cells of the MCF-7 line under the glycoside action (Figure 4e).

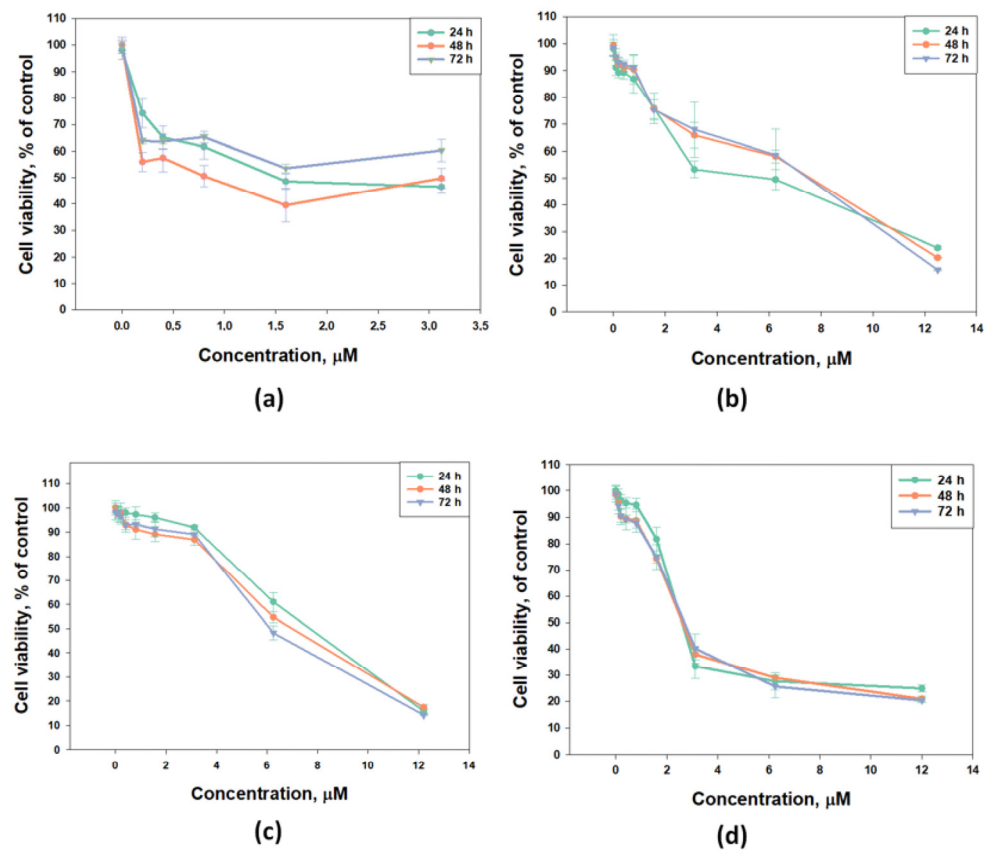


Figure 2. Cytotoxic effect of glycosides against breast cancer cells: (a) djakonovioside E₁ (3) against MCF-7, (b) cucumarioside A₂-5 (6) against T-47D cells, (c) djakonovioside C₁ (1) against MDA-MB-231 cells, and (d) cucumarioside A₂-5 (6) against MDA-MB-231 cells for 24 h, 48 h, and 72 h. All experiments were carried out in triplicate. The data are presented as mean ± SEM.

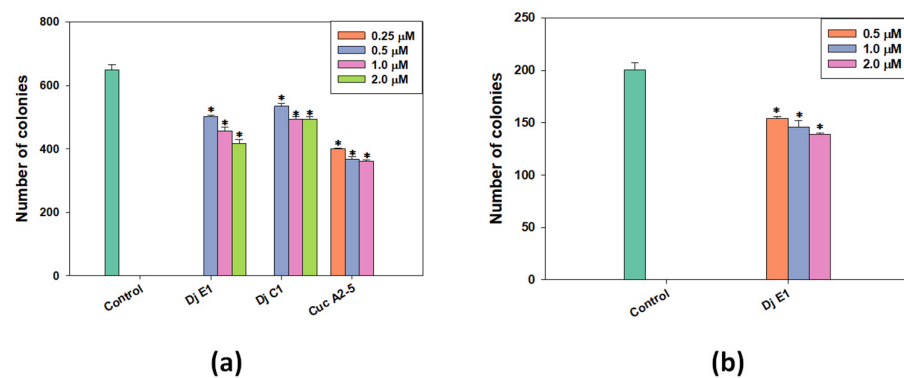


Figure 3. The number of MDA-MB-231 (a) and MCF-7 (b) cell colonies under the treatment with different concentrations of djakonovioside C₁ (1), djakonovioside E₁ (3), and cucumarioside A₂-5 (6). ImageJ 1.52 software was used to count the cell colonies. Data are presented as means ± SEM. * *p* value ≤ 0.05 considered significant.

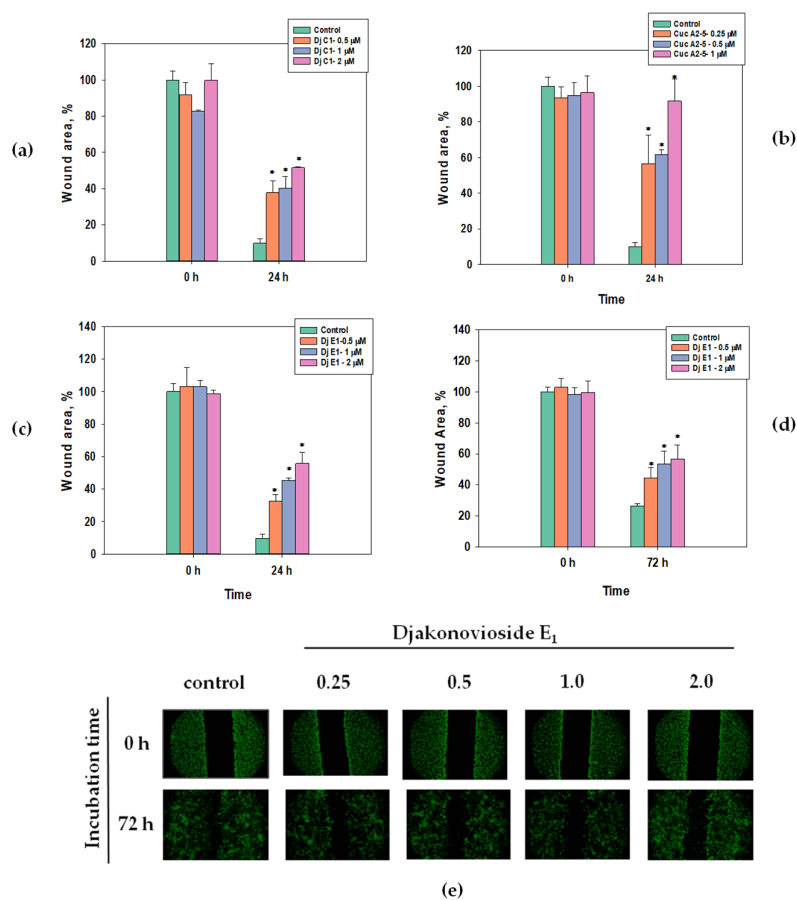


Figure 4. Migration of MDA-MB-231 and MCF-7 cells into wound areas observed with MIB-2-FL fluorescence microscope at 10-fold magnification: (a) MDA-MB-231 cells 0 and 24 h after treatment with 0.5, 1.0, and 2.0 μM of djakonovioside C₁ (1); (b) MDA-MB-231 cells 0 and 24 h after treatment with 0.25, 0.5, and 1.0 μM of cucumarioside A₂-5 (6); (c) MDA-MB-231 cells 0 and 24 h after treatment with 0.5, 1.0, and 2.0 μM of djakonovioside E₁ (3); (d,e) MCF-7 cells 0 and 72 h after treatment with 0.5, 1.0, and 2.0 μM of djakonovioside E₁ (3). Cells were stained with the fluorescent dye CFDA SE. Cell migration into wound areas processed by ImageJ 1.52 software. Data are presented as means \pm SEM. * p value \leq 0.05 considered significant.

2.3. Correlational Analysis and QSAR Model

The quantitative structure–activity relationship (QSAR) approach was applied to analyze the correlation between the hemolytic activity values and structures of all the glycosides isolated from *C. djakonovi*. Three-dimensional models of the glycosides were built, protonated at pH 7.4, and subjected to energy minimization. A conformational search was performed with MOE 2020.0901 CCG software [22], and the dominant glycoside conformations were selected for further analysis. A set of various 2D and 3D descriptors (379 in total) responsible for physicochemical properties, as well as energy values and topological indexes numerically expressing the geometric properties of molecular structures, was calculated and analyzed using the QuaSAR-Descriptor tool of the MOE 2020.0901 CCG software [22].

Noticeably, the descriptors choice has a fundamental significance, since no “almighty descriptor set” modeling all the activities and properties has been found yet. So, the selection of a suitable descriptor set for each activity and type of analyzed compounds is needed. So, in addition to the descriptors characterizing the physicochemical properties of the molecules (polarizability, refractive index, surface charge distribution, dipole moment, hydrogen bonds’ potential strength (donors and acceptors) [23], hydrophobic volume, surface area, atomic valence connectivity index, etc.), following descriptors as the

presence/absence of 18(20)-lactone and the side chain, carbohydrate chain branching, and nature of the second sugar residue (glucose, quinovose, and xylose), the sulfate groups' number and positions were added to the descriptors set provided by the MOE-QuaSAR-Descriptor software (2020.0901 CCG). The correlational analysis revealed the direct positive correlation between the hemolytic activities of the tested compounds in vitro and such descriptors as the molecular refractivity, log of the octanol/water partition coefficient [24], and partial charges distribution on the van der Waals surface area. In contrast, the diameter of the molecule, principal moment of inertia describing the different aspects of molecular shape, VDW surface area (\AA^2), molecular VDW volume (\AA^3), lowest hydrophobic energy, and approximation of the sum of the VDW surface areas of hydrophobic atoms (\AA^2) were found to negatively correlate.

The analysis of the principal components (PCA) decreased the number of descriptors, leaving only those having a substantial contribution, and resulted in the division of the glycosides into two groups (Figure 5), which indicated the right way of the descriptor's choice. The linear QSAR model was built with the QuaSAR-Model tool of the MOE 2020.0901 CCG software [22] using these descriptors. The model fits well with the experimental data on the hemolytic activities of glycosides with a correlation coefficient $r^2 = 0.94702$ and $\text{RMSE} = 0.05234$ (Figure S58). The model was cross-validated with $r^2_{\text{cross}} = 0.82341$ and $\text{RMSE}_{\text{cross}} = 0.24613$. The QSAR model includes 148 terms, 58 from those that have the biggest contribution; however, the reduction in the number of descriptors to the latter value resulted in the quality deterioration of the correlation model. All these data indicate the extremely complex nature of the relationships between the structure of glycosides and their membranolytic action, with the multiple negligible effects of plenty of descriptors causing a considerable effect in combination with each other.

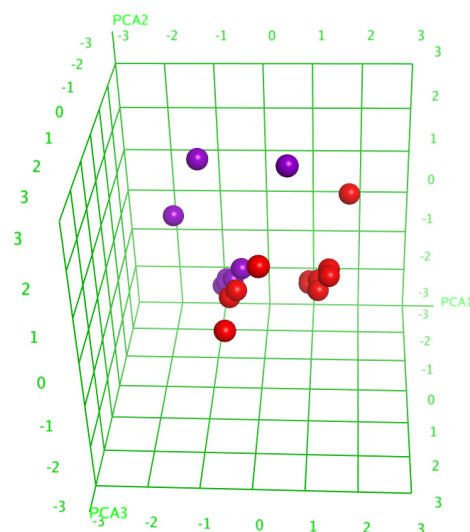


Figure 5. Three-dimensional plot of hemolytic activity (pED_{50}) depending on the principal components' values (PCA1—PCA3) calculated for 20 glycosides. The glycosides that demonstrated hemolytic activity with $\text{ED}_{50} \leq 10 \mu\text{M}$ were outlined as active and are marked in red, while the rest are marked in violet.

3. Discussion

3.1. Analysis of Structural Peculiarities of Glycosides: Significance for Chemotaxonomy and Biogenesis

Six compounds (1–3 and 5–7) from the last series of glycosides isolated from *C. djakonovi* contained four different holostane-type aglycones. The aglycone of new djakonoviosides C_1 (1), and E_1 (3) and known okhotoside A_2 -1 (5) was found earlier in the glycosides of sea cucumbers *C. japonica* [25], *Neothyonidium magnum* [26], and *Thyone aurea* [27]. The aglycone of djakonovioside D_1 (2) is present in plenty of glycosides from different species of sea cucumbers [15,28–33]. The aglycone of known cucumarioside A_2 -5 (6) was also revealed in okhotoside A_1 -1 [18] and cucumarioside A_0 -1 [34] isolated earlier from *C. djakonovi* [5]. The

aglycone of frondoside A₂-3 (7)—the glycoside of *C. frondosa* [20]—characterized by the absence of any substituents at C-16 as well as by the differing side chain structure is not so common. It was repeatedly found only in chitonoidoside K₁ from *Psolus chitonoides* [35]. All these aglycones are characterized by the presence of a 7(8)-double bond, being the products of one oxidosqualenecyclase (OSC).

Four reported glycosides (4 and 8–10) contained non-holostane aglycones without a lactone ring, including a new one in djakonovioside F₁ (4). Noticeably, djakonovioside F₁ (4) is the only compound from this row having a normal non-shortened side chain. The other three aglycones are hexa-*nor*-lanostane derivatives. Djakonovioside F₁ (4), cucumaroside A₃-2 (8), and koreoside A (10) formed a biogenetic row reflecting the formation in the process of the biosynthesis of *nor*-lanostane derivatives through the stage of C-22 oxidation and following the oxidative cleavage of the 20(22)-covalent bond. This leads to the elimination of a side chain. The same way is realized during the biosynthesis of steroid hormones. Remarkably, the set of trisulfated pentaosides of *C. djakonovi* (djakonovioside F₁ (4), isokoreoside A (9), and koreoside A (10)) complements and resembles the analogical set found in *C. frondosa* [17]: three pairs of isomers differed by the positions of the double bonds in the lanostane nuclei had a differently substituted C-22 or a shortened side chain. Compound 4, having a carbonyl group at C-22, can be considered as a missing link in the row of aglycones of the *C. frondosa* glycosides that fills the gap between the 22-hydroxylated (22-*O*-acetylated) and hexa-*nor*-lanostane derivatives.

Interestingly, isokoreoside A (9) is the single glycoside from *C. djakonovi* having a 9(11)-double bond. This indicates that two oxidosqualenecyclases (OSCs) (parkeol syntase and 9 β H-lanosta-7,24-diene-3 β -ol syntase) are operating in the biosynthesis and forming different types of polycyclic nuclei of the glycosides of *C. djakonovi*. However, the parkeol syntase seems to be preferably engaged in the biosynthesis of free 14 α -methyl sterols with a 9(11)-double bond, while the 9 β H-lanosta-7,24-diene-3 β -ol synthase's action leads to triterpene aglycones' formation. Recent investigations into sea cucumber glycosides showed that some species contain mainly one type of aglycones with a certain position of intranuclear double bond, but the others accumulate glycosides with different positions for the double bonds in the polycyclic system [4]. However, even when glycosides preferably contain aglycones with one position of the intranuclear double bond, for example, $\Delta^{7(8)}$ -aglycones in *E. fraudatrix* [36] and *S. horrens* [37] and $\Delta^{9(11)}$ -aglycones in *A. japonicus* [38], the genes of at least two OSCs are expressed, albeit with different efficiencies. In *C. djakonovi*, the situation seems to be different: the level of expression of parkeol syntase and its activity is obviously on the high level; however, the major part of biosynthesized parkeol is subsequently used for the formation of 14 α -methylsterols with a 9(11)-double bond. Such parkeol-derived sterols are very typical for sea cucumbers belonging to the order Dendrochirotida, including the family Cucumariidae [39–43].

Generally, five new aglycones were found in the glycosides isolated from *C. djakonovi* [5]. Noticeably, the new aglycones are mainly inherent for monosulfated compounds, while, among trisulfated compounds, only one glycoside having a novel aglycone was discovered. Eight types of carbohydrate chains comprised the glycosides of *C. djakonovi*. Two sugar chains, known earlier from the glycosides of *C. okhotensis* [18], *C. japonica* [34], and *C. frondosa* [44,45], are the parts of the djakonoviosides of groups A and B (monosulfated tetra- and pentaosides, with second quinovose and third xylose residues). Among the last series of glycosides from *C. djakonovi*, two types of carbohydrate moieties were found for the first time, while four were known earlier. The monosulfated pentasaccharide chain of djakonovioside C₁ (1), with xylose as the second unit, was new. Such a structural feature is very rare for holothurios glycosides. It was only found in two of several hundred compounds known from representatives of the order Dendrochirotida [46,47]. Additionally, the trisulfated tetrasaccharide chain of djakonovioside E₁ (3), with glucose as the second unit, was revealed first. The oligosaccharide parts of djakonoviosides D₁ (2) and F₁ (4) and known compounds 5–10 are also characteristic for other representatives of the *Cucumaria* genus: *C. okhotensis* [18], *C. conicospermium* [19], *C. frondosa* [17,20], *C. japonica* [48], and

C. koreensis [21]. These data confirm the possibility of using glycosides as chemotaxonomic markers. Belonging to *C. djakonovi* to the genus *Cucumaria* is undoubtedly evidenced by the presence of the same glycosides, characteristic to the other species of the genus. The supposition that all *Cucumaria* species share the same mono-, di-, and trisulfated pentasaccharide branched chains and species-specific aglycones is corroborated by the structures of *C. djakonovi* glycosides [14]. However, the set of sugar chains biosynthesized by sea cucumbers of the *Cucumaria* genus is broadened with novel oligosaccharide moieties.

Biogenetic analysis of sugar chain structures of *C. djakonovi* glycosides showed that each type of carbohydrate chain is formed by a single way, including glycosylation with a certain monosaccharide residue or sulfation reactions. The branching of pathways occurs at the stage of glycosylation of the monoxylosides with additional xylose (forming the djakonovioside C₁ (1) chain), quinovose, or glucose residues (Figure 6). Subsequently the pathway of the biosynthesis of quinovose-containing glycosides divides depending on the type of third monosaccharide (xylose or glucose), which glycosylates quinovose residue by C-4. At this stage, tetrasaccharide chains of the djakonoviosides of group A are formed. Next, branching with xylose leads to the djakonoviosides of group B. In the case of glycosides having glucose as the third sugar, the tetrasaccharide precursors are obviously initially subjected to glycosylation, forming the pentasaccharide chains of cucumarioside A₂-5 (6) and frondoside A₂-3 (7), followed by further sulfation leading to disulfated cucumarioside A₃-2 (8) and trisulfated djakonovioside F₁ (4), isokoreoside A (9), and koreoside A (10).

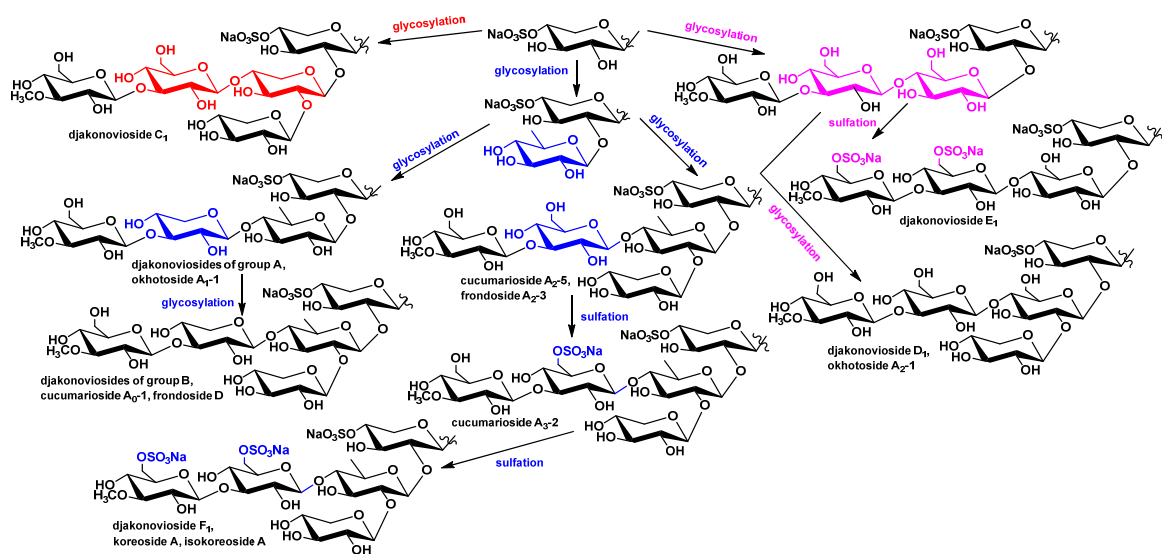


Figure 6. The scheme of biosynthesis of carbohydrate chains of the glycosides of *C. djakonovi*.

The third direction of sugar chains' biosynthesis is realized when the glucose glycosylates monoxylosides. The next steps of the chain's elongation are glycosylation with glucose and 3-O-methylglucose (third and fourth residues). Then, two pathways are possible: the two stages of sulfation resulting in the chain of djakonovioside F₁ (4) or the glycosylation of the C-2 position of Glc2 leading to the chain of djakonovioside D₁ (2).

So, the biosynthesis of the carbohydrate moieties of *C. djakonovi* glycosides looks rather strictly directed, in comparison with that of the aglycones, exhibiting the time shifts of some stages that is typical for the mosaic type of biosynthesis. The mosaicism of the biosynthesis of the glycosides of *C. djakonovi* clearly appeared at the level of the whole molecules as the combination of different sugar moieties with the same aglycones, due to the parallel and independent biosynthesis of these parts of molecules. There are some examples: cucumariosides A₂-5 (6) and A₀-1 and okhotoside A₁-1 [5], as well as djakonoviosides C₁ (1) and E₁ (3) and okhotoside A₂-1 (5), share the same aglycone.

It is interesting that hexa-*nor*-lanostane glycosides, structurally similar to sex (steroid) hormones, are mainly trisulfated or rarely disulfated (the biosynthetic precursors of trisulfated) compounds in the representatives of the genus *Cucumaria* [17,19,21], including *C. djakonovi*. These data, along with the metabolite profiling of a representative of the family Sclerodactylidae—the sea cucumber *Eupentacta fraudatrix* [10], where *nor*-lanostane derivatives were quantitatively predominant in the gonads—probably indicate that the role of such metabolites is different from that of the other glycosides, which provide the chemical defense of sea cucumbers. Actually, it is known that glycosides also synchronize the oocyte maturation in the holothurians population. So, a high level of sulfation makes them more polar and hydrophilic and facilitates their release into the surrounding sea water. Such an exchange with chemical signals provides the simultaneous readiness to spawn all the animals in the population.

3.2. Tendencies of Biologic Activity of the Glycosides: Observed and Calculated Structure Activity Relationships (SAR and QSAR)

The observed structure–activity relationships based on the hemolytic activity demonstrated that the most active compounds, okhotoside A₂-1 (5) and cucumarioside A₂-5 (6), from the tested series have holostane-type aglycones and monosulphated pentasaccharide chains. The high hemolytic effect of djakonovioside F₁ (4) was unexpected due to the absence of a lactone in 4 and the presence of three sulfate groups. The presence of a 22-keto group in the side chain of 4 in close proximity to the 20-OH group obviously resulted in the intramolecular hydrogen bond formation leading to a spatial structure similar to the lactone ring that resulted in the increase of the activity. Djakonovioside C₁ (1), having the same aglycone as okhotoside A₂-1 (5), showed slightly lower activity due to the presence of xylose as the second residue of the sugar chain. Djakonovioside D₁ (2), being isomeric to 5 by the double bond position in the side chain, also was slightly less hemolytic. The absence of the activity of frondoside A₂-3 (7) is easily explained by the presence of a hydroxy group in its side chain [15]. The low hemolytic activity of cucumarioside A₃-2 (8) and isokoreoside A (9) is determined by the presence of non-holostane aglycones with shortened side chains; the same features led to the complete loss of the activity of koreoside A (10). The partial compensation of the hemolytic action of 8 and 9, in comparison with compound 10, was presumably realized due to the presence of two sulfate groups instead of three in 8 and the 9(11)-position of the intranuclear double bond in 9. Erythrocytes were, as usual, more sensitive to the membranolytic action of glycosides than cancer cells.

Quantitative structure–activity relationships were calculated on the basis of correlational analysis of the physicochemical properties and structural features of the glycosidic molecules and their membranolytic activity and revealed the extremely complex nature of such relationships. The characteristics of molecules related with charged groups, such as polarization under the influence of the electric fields of neighboring ions, surface charge distribution, and impact of hydrophobic/hydrophilic areas and some others considerably influence the membranotropic activity of glycosides. The discovered dependence of the activity upon such chemical peculiarities as the number and positions of double bonds, single bond chain (aglycone side chain) length, availability of 18(20)-lactone, branching and monosaccharide composition of the carbohydrate chain, and positions and numbers of sulfate groups logically follows from the above physical characteristics. More importantly, the QSAR results are consistent with the observed structure–activity relationships. Actually, the availability of a normal non-shortened side chain is urgently needed for the glycoside to be active (i.e., hexa-*nor*-lanostane compounds 8–10 are almost not active). The presence of 18(20)-lactone also provides significant activity, as illustrated not only by *C. djakonovi* glycosides [5] but also is a common tendency [15]. The negative correlation of the molecular volume and shape with the hemolytic activity is confirmed by the observation that tetraosides with linear carbohydrate chains showed stronger effects than the corresponding pentaosides [5,15]. The calculations showed that the number of sulfate groups has an ambiguous effect on the activity of the tested glycosides. In this case, the

calculations are also backed with observations: disulfated cucumarioside A₃-2 (8) is more active than trisulfated koreoside A (10). The presence of a third sulfate group, unlike the second one, is not conducive to the membranotropic properties of the analyzed glycosides. It should be noted that the influence of sulfate groups on the membranolytic action of the triterpene glycosides depends on the architecture of their carbohydrate chains and the positions of attachment of these functional groups. Hence, increasing the numbers of sulfates in the glycosides with tetrasaccharide and pentasaccharide chains branched by the C-2 of quinovose leads to the activity decreasing [15], which is in good accordance with the observations: trisulfated tetraoside djakonovioside E₁ (3) is weakly hemolytic. So, the complicated and ambiguous character of structure–activity relationships is related to the diverse impact on the membranolytic action of certain structural elements and their combinations in the glycosidic molecules.

Regarding the cytotoxicity of the tested compounds against human breast cancer cells, the selective action of djakonovioside E₁ (3) against the ER-positive MCF-7 cell line and the triple-negative MDA-MB-231 cell line, which fail to express receptors to sex hormones and have no approved targeted therapeutics, was the most important finding, especially amid the absence of a toxic effect in relation to normal mammary epithelial cells (MCF-10A) and low hemolytic activity. The MDA-MB-231 (triple-negative breast cancer) cell line was the most sensitive to cytotoxic action, while the MCF-7 cell line was the most resistant.

The action of djakonoviosides C₁ (1), E₁ (3), and cucumarioside A₂-5 (6), which are the most active against cancer cells, was more deeply studied. It was shown that these compounds did not lose cytotoxicity over time, and djakonovioside E₁ (3) demonstrated an antiproliferative effect. The compounds were able to inhibit colony formation and growth in selected cell lines, with cucumarioside A₂-5 (6) demonstrating the greatest inhibitory effect. The same glycoside was the strongest inhibitor of tumor cell migration. The other glycosides also reliably suppressed cell motility. Such properties of the studied glycosides corroborate their potential to be used as anticancer agents.

4. Materials and Methods

4.1. General Experimental Procedures

PerkinElmer 343 Polarimeter (PerkinElmer, Waltham, MA, USA) was used for specific rotation measuring; NMR spectra were registered on Bruker AMX 500 (Bruker BioSpin GmbH, Rheinstetten, Germany) (500.12/125.67 MHz (¹H/¹³C) spectrometer; ESI MS (positive and negative ion modes) spectra were obtained on Agilent 6510 Q-TOF apparatus (Agilent Technology, Santa Clara, CA, USA), sample concentration 0.01 mg/mL; HPLC was conducted on Agilent 1260 Infinity II equipped with a differential refractometer (Agilent Technology, Santa Clara, CA, USA); columns were used: Phenomenex Synergi Fusion RP (10 × 250 mm) and Synergi Hydro RP (10 × 250 mm) (Phenomenex, Torrance, CA, USA) (flow rate 1.5 mL/min), as well as chiral analytical column Kromasil 3-Cellucoat RP (4.6 × 150 mm) (Nouryon HQ, Amsterdam, the Netherlands) (flow rate of 0.5 mL/min).

4.2. Animals and Cells

The specimens of sea cucumber *Cucumaria djakonovi* (family Cucumariidae; order Dendrochirotrida) were gathered by scuba diving from a depth of 14–15 m near Starichkov's Island (Avacha Gulf) in July 2007. The taxonomic identification of the animals was performed by Stepanov V.G. Voucher specimen is kept in the Pacific Institute of Geography, Kamchatka Branch, Petropavlovsk-Kamchatsky, Russia.

Human erythrocytes were purchased from the Station of Blood Transfusion, Vladivostok. Human mammary epithelial cell line MCF-10A CRL-10317, human breast cancer cell lines T-47D HTB-133, MCF-7 HTB-22, and MDA-MB-231 CRM-HTB-26 were received from ATCC (Manassas, VA, USA). Culturing conditions: medium of RPMI-1640 with 1% penicillin/streptomycin (Biolot, St. Petersburg, Russia) and 10% fetal bovine serum (FBS) (Biolot, St. Petersburg, Russia) for T-47D cell line; Minimum Essential Medium (MEM) with 1% penicillin/streptomycin sulfate (Biolot, St. Petersburg, Russia) and FBS (Biolot,

St. Petersburg, Russia) to a final concentration of 10% for MCF-7 and MDA-MB-231 cells; DMEM/F12 medium with 10% FBS, 20 ng/mL EGF, 0.5 mg/mL hydrocortisone, 100 ng/mL cholera toxin, 10 µg/mL insulin, and 1% penicillin/streptomycin (Bioinnlabs, Russia) for MCF-10A cell line.

4.3. Extraction and Isolation

The raw material of the sea cucumbers (663.5 g) was obtained after twice extracting with refluxing 70% EtOH. The extract, dissolved in H₂O, was chromatographed on a Polychrom-1 column (powdered Teflon, Biolar, Latvia) for the elimination of inorganic salts and impurities. Crude glycoside fraction (1379 mg) was obtained as result of elution with 55% acetone. Its separation by chromatography on Si gel columns (CC) with the stepped gradient of the system of eluents of CHCl₃/EtOH/H₂O in ratios of 100:50:4, 100:75:10, 100:100:17, and 100:125:25 gave five fractions. The fractions III, IV, and V were subjected to additional stage of CC with the system of eluents of CHCl₃/EtOH/H₂O (100:75:10), (100:100:17), and (100:125:25) that led to isolation of subfractions 3 (262 mg), 4 (1154 mg), and 5 (820 mg), respectively. HPLC of subfraction 3 on reversed-phase column Synergi Fusion RP (10 × 250 mm) with MeOH/H₂O/NH₄OAc (1M water solution) in ratio of (68/30/2) as mobile phase gave fractions 3(1)–3(8). The re-chromatography of fractions 3(8) with CH₃CN/H₂O/NH₄OAc (1M water solution) (40/58/2) as mobile phase resulted in the isolation of djakonovioside D₁ (2) (3.6 mg, Rt 17.5 min); 3(7) and 3(5) with CH₃CN/H₂O/NH₄OAc (1M water solution) (39/59/2) gave djakonovioside C₁ (1) (8 mg, Rt 21.2 min), okhotoside A₂-1 (5) (5.6 mg, Rt 18.7 min) from 3(7), and cucumarioside A₂-5 (6) (7 mg, Rt 17.2 min) from 3(5); 3(4) with CH₃CN/H₂O/NH₄OAc (1M water solution) (34/64/2) resulted in the isolation of frondoside A₂-3 (7) (3.3 mg, Rt 15.1 min). Subfraction 4 was subjected to HPLC on the same column with CH₃CN/H₂O/NH₄OAc (1M water solution) (34/64/2) as mobile phase and was separated to two main fractions. One of them was subsequently submitted to HPLC on the Kromasil 3-Cellucoat RP (4.6 × 150 mm) column with CH₃CN/H₂O/NH₄OAc (1M water solution) (20/78/2) as mobile phase to give individual djakonovioside E₁ (3) (5 mg, Rt 11.9 min). From another fraction, cucumarioside A₃-2 (8) (3.1 mg, Rt 15.3 min) was isolated as result of HPLC on Synergi Hydro RP column (10 × 250 mm) with MeOH/H₂O/NH₄OAc (1M water solution) in ratio of (67/29/4). The separation of subfraction 5 on Synergi Hydro RP column (10 × 250 mm) with MeOH/H₂O/NH₄OAc (1M water solution) in ratio of (66/30/4) gave isokoreoside A (9) (3.4 mg, Rt 13.0 min), koreoside A (10) (3.4 mg, Rt 12.1 min), and djakonovioside F₁ (4) (4.0 mg, Rt 18.4 min).

4.3.1. Djakonovioside C₁ (1)

Colorless powder; $[\alpha]_D^{20} -45^\circ$ (c 0.1, H₂O), mp 215 °C. NMR: Tables 1 and 2, Figures S1–S8. (–)HR-ESI-MS *m/z*: 1325.5451 (calc. 1325.5478) [M_{Na} – Na][–]; (–)ESI-MS/MS *m/z*: 1265.5 [M_{Na} – Na – CH₃COOH][–], 1223.5 [M_{Na} – Na – NaSO₃ + H][–], 1193.5 [M_{Na} – Na – Xyl (C₅H₈O₄)][–], 987.4 [M_{Na} – Na – MeGlc (C₇H₁₂O₅) – Glc (C₆H₁₀O₅) + H][–], 813.2 [M_{Na} – Na – Agl (C₃₂H₄₇O₅) – H][–], 681.1 [M_{Na} – Na – Agl (C₃₂H₄₇O₅) – Xyl (C₅H₉O₄)][–], 595.2 [M_{Na} – Na – Agl (C₃₂H₄₇O₅) – XylSO₃ (C₅H₇O₆SNa)][–]; (+)ESI-MS/MS *m/z*: 1251.6 [M_{Na} + Na – NaHSO₄]⁺, 1179.6 [M_{Na} + Na – MeGlc (C₇H₁₃O₆) + H]⁺.

4.3.2. Djakonovioside D₁ (2)

Colorless powder; $[\alpha]_D^{20} -53^\circ$ (c 0.1, H₂O), mp 219 °C. NMR: Tables 3 and 4, Figures S9–S16. (–)HR-ESI-MS *m/z*: 1355.5596 (calc. 1355.5584) [M_{Na} – Na][–], 677.2767 (calc. 677.2755) [M_{Na} – Na – H]^{2–}; (–)ESI-MS/MS *m/z*: 1296.5 [M_{Na} – Na – CH₃COOH][–], 1105.5 [M_{Na} – Na – SO₃Na – Xyl (C₅H₉O₅) + H][–], 843.2 [M_{Na} – Na – Agl (C₃₂H₄₇O₅) – H][–], 723.3 [M_{Na} – Na – Agl (C₃₂H₄₇O₅) – NaSO₄][–], 589.2 [M_{Na} – Na – MeGlc (C₇H₁₃O₅)]^{2–}; (+)ESI-MS/MS *m/z*: 1281.6 [M_{Na} + Na – NaHSO₄]⁺, 1209.6 [M_{Na} + Na – MeGlc (C₇H₁₃O₆) + H]⁺.

4.3.3. Djakonovioside E₁ (3)

Colorless powder; $[\alpha]_D^{20} - 50^\circ$ (*c* 0.1, H₂O), mp 204 °C. NMR: Tables 5 and S1, Figures S17–S24. (–)HR-ESI-MS *m/z*: 1427.3942 (calc. 1427.3936) [M_{3Na} – Na][–]; 702.2037 (calc. 702.2022) [M_{3Na} – 2Na]^{2–}; 460.4732 (calc. 460.4717) [M_{3Na} – 3Na]^{3–}; (–)ESI-MS/MS *m/z*: 1367.4 [M_{3Na} – Na – CH₃COOH][–], 1307.4 [M_{3Na} – Na – NaHSO₄][–], 1029.4 [M_{3Na} – Na – NaHSO₄–MeGlcSO₃ (C₇H₁₂O₉SNa) + H][–], 915.1 [M_{3Na} – Na – Agl (C₃₂H₄₇O₅) – H][–], 681.1 [M_{3Na} – Na – Agl (C₃₂H₄₇O₅) – XylSO₃ (C₅H₇O₇SNa) – H][–], 519.0 [M_{3Na} – Na – Agl (C₃₂H₄₇O₅) – XylSO₃ (C₅H₇O₇SNa) – Glc (C₆H₁₀O₅) – H][–], 446.0 [M_{3Na} – 2Na – Agl (C₃₂H₄₇O₅) – H]^{2–}.

4.3.4. Djakonovioside F₁ (4)

Colorless powder; $[\alpha]_D^{20} - 32^\circ$ (*c* 0.1, H₂O), mp 196 °C. NMR: Tables 6 and 7, Figures S25–S32. (–)HR-ESI-MS *m/z*: 1487.4467 (calc. 1487.4511) [M_{3Na} – Na][–], 732.2320 (calc. 732.2310) [M_{3Na} – 2Na]^{2–}, 480.4926 (calc. 480.4909) [M_{3Na} – 3Na]^{3–}; (–)ESI-MS/MS *m/z*: 1489.5 [M_{3Na} – Na + 2][–], 1211.4 [M_{3Na} – Na + 2 – MeGlcSO₃ (C₇H₁₁O₈SNa)][–], 947.4 [M_{3Na} – Na + 2 – MeGlcSO₃ (C₇H₁₁O₈SNa) – Glc SO₃ (C₆H₉O₈SNa)][–], 797.1 [M_{3Na} – Na + 2 – MeGlcSO₃ (C₇H₁₁O₈SNa) – Glc SO₃ (C₆H₉O₈SNa) – XylSO₃ (C₅H₉O₅) – H][–].

4.4. Cytotoxic Activity (MTT Assay)

The concentrations of tested glycosides were 0.1–50 μM; positive controls—cisplatin and djakonovioside A₁ [5]. Methodology: to each well of 96-well plates, the cell suspension (180 μL) with solution (20 μL) of tested glycoside in the certain concentration was placed (MCF-10A, MCF-7, T-47D, and MDA-MB-231—7 × 10³ cells per well) and incubated in the atmosphere with 5% CO₂ at 37 °C for 24 h. The times of incubation of cucumarioside A₂-5 (6) and djakonoviosides C₁ (1) and E₁ (3), at concentrations of 0.5–12.0 μM with T-47D, MCF-7, or MDA-MB-231 cells, were 24, 48, and 72 hrs. Then, the solutions of tested compounds with medium were replaced by 100 μL of fresh medium, and 10 μL of 3-(4,5-dimethylthiazol-2-yl)-2,5-diphenyltetrazolium bromide (MTT) (PanReac, AppliChem, Darmstadt, Germany) stock solution (5 mg/mL) was added to each well and incubated for 4 h, followed by the addition of 100 μL of SDS-HCl solution (1 g SDS/10 mL d-H₂O/17 μL 6 N HCl) and further incubated for 18 h. Multiskan FC microplate photometer (Thermo Fisher Scientific, Waltham, MA, USA) was used to measure the absorbance of the converted dye formazan at 570 nm. The concentration caused 50% cell metabolic activity inhibition (IC₅₀), which expresses the cytotoxic activity of each glycoside. The experiments were conducted in triplicate, *p* ≤ 0.05.

4.5. Hemolytic Activity

Human blood (B(III) Rh+) was used to obtain erythrocytes by centrifuging 450 × *g* three times for 5 min with phosphate-buffered saline (PBS) (pH 7.4) at 4 °C on centrifuge LABOFUGE 400R (Heraeus, Hanau, Germany). Ice-cold PBS (pH 7.4) was used for resuspension of erythrocytes residue to a final optical density of 1.5 at 700 nm, which was kept on ice. Then, 20 μL of tested compound solution or control—djakonovioside A₁ [5]—were added to 180 μL of erythrocyte suspension in V-bottom 96-well plates and exposed for 1 h at 37 °C. Next, centrifugation at 900 × *g* for 10 min on laboratory centrifuge LMC-3000 (Biosan, Riga, Latvia), led to layers' separation, and 100 μL of supernatant was carefully decanted and transferred into new flat-plate each. The values of erythrocyte lysis were measured on microplate photometer Multiskan FC (Thermo Fisher Scientific, Waltham, MA, USA) at λ = 570 nm as hemoglobin concentration in supernatant. The effective dose, causing lysis of 50% erythrocytes (ED₅₀), was calculated with SigmaPlot 14.0 software. All the experiments were carried out in triple repetitions, *p* ≤ 0.05.

4.6. Colony Formation Assay

The influence of glycosides on colony formation by MCF-7 or MDA-MB-231 cells was tested by the clonogenic assay [49]. Cell density: 1 × 10³ for MDA-MB-231 and 0.3 × 10³

for MCF-7 cells per well; cell culture: MEM media, 10% FBS, 10,000 U/mL of penicillin, and 10,000 µg/mL of streptomycin supplemented or not (control) with different concentration of glycosides; incubation conditions: 10 days, 37 °C, atmosphere with 5% CO₂; obtained: visible to eye colonies (at least 50 cells per colony); fixation with methanol (25 min); staining with 0.5% solution of crystal violet (25 min); washing and air-drying of plates.

4.7. Wound Scratch Migration Assay

Attached to special migration plate plastic bottom MCF-7 or MDA-MB-231 cells were separated by a silicone insert (Culture-insert 2 Well 24, ibiTreat). After removing an insert, gap between the cells was 500 ± 50 µm. Cell debris and floating cells were deleted by washing twice with PBS; 10 µM of 5 mM initial solution of CFDA SE ((5,6)-carboxyfluorescein succinimidyl ester) (LumiTrace CFDA SE kit, Lumiprobe, Moscow, Russia) in DMSO was dissolved in PBS and added to cells for 5 min at 37 °C; after washing twice with PBS, the fresh culture medium was added. Then, cells were treated with various concentrations of glycosides or culture medium only (vehicle control) and left for 24 and 72 h. Cell migration into the wound area was observed under a fluorescence microscope (MIB-2-FL, LOMO, Russia) with objective 10× magnification.

4.8. Building a QSAR Model

QSAR model for the set of 20 glycosides was built using QuaSAR-Descriptor and QuaSAR-Model tools of MOE 2020.0901 software [22]. The procedure involved the following steps: a charge calculation and structure optimization, glycosides conformational search, descriptors calculation, correlational analysis, principal component analysis (PCA), removing the descriptors collinear with another descriptor (unnecessary descriptors), building a QSAR model and the model's cross-validation, removing the descriptors not contributing to the model, and model checking by making a graph showing the correlation between the model-predicted value and the experimental activity value expressed as pED₅₀.

5. Conclusions

As result of thorough research on the glycosidic composition of the sea cucumber *Cucumaria djakonovi*, 11 new djakonoviosides and 9 known glycosides, found earlier in other representatives of the *Cucumaria* genus, were isolated in general. Twelve different aglycones were the parts of the found compounds, and five of them were new ones, including a unique one having a 2,3,16-hemiketal fragment. Nine types of carbohydrate chains composed the glycosides of *C. djakonovi*. Two types of sugar moieties were revealed first, including those with xylose or glucose residue in the second position of the chain.

The pathways of biosynthesis of the aglycones and carbohydrate moieties of *C. djakonovi*'s glycosides were proposed, showing the regularities characteristic of the mosaic type of biosynthesis.

It was shown that, on the one hand, the unique species-specific composition of the glycosides is inherent for each species of the genus *Cucumaria*, and, on the other hand, the presence of some common glycosides for all representatives of the genus is typical.

Some of the glycosides from *C. djakonovi* display promising anti-breast-cancer effects expressed as the inhibition of cells' viability, functioning, and motility—the aspects of carcinogenesis occurring in the organism.

Quantitative structure–activity relationships analysis confirmed the complicated, tricky character of these correlations because of the influence on the activity of a large number of properties and peculiarities of the molecules that act in combination altogether. Importantly, the calculated results of QSAR are in good accordance with the observed SAR, concluded on the basis of the experimental data. All these indicate that the application of this instrument for the prediction or modeling of the biologic activity of sea cucumbers' triterpene glycosides is rather prospective and useful.

Supplementary Materials: The following supporting information can be downloaded at <https://www.mdpi.com/article/10.3390/md21120602/s1>. Figures S1–S58: The original spectral data of compounds 1–10; Tables S1–S9: ^{13}C and ^1H NMR chemical shifts and HMBC and ROESY correlations of carbohydrate moieties or the aglycones of glycosides 3, 5–7, 9, and 10; the PCR QSAR model correlation plot.

Author Contributions: Conceptualization, A.S.S. and V.I.K.; investigation, A.S.S., S.A.A., A.I.K., R.S.P., P.S.D., E.A.C., E.S.M., E.A.Z., E.G.P. and V.G.S.; methodology, A.S.S., E.A.C. and E.S.M.; writing—original draft, A.S.S.; supervision, P.S.D.; review and editing, V.I.K. All authors have read and agreed to the published version of the manuscript.

Funding: The investigation was conducted with the financial support of a grant from the Russian Science Foundation, no. 23-13-00078.

Institutional Review Board Statement: Not applicable.

Data Availability Statement: The original data presented in the study are included in the article/Supplementary Materials.

Acknowledgments: The study was carried out on the equipment of the Collective Facilities Center “The Far Eastern Center for Structural Molecular Research (NMR/MS) PIBOC FEB RAS”; the computer simulation and conformational search for glycosides were performed using the cluster CCU “Far Eastern computing resource” FEB RAS (Vladivostok).

Conflicts of Interest: The authors declare no conflict of interest.

References

1. Chanley, J.D.; Mezzetti, T.; Sobotka, H. The holothurinogenins. *Tetrahedron* **1966**, *22*, 1857–1884. [[CrossRef](#)]
2. Habermehl, G.G.; Krebs, H.C. Toxins of echinoderms. In *Studies in Natural Products Chemistry*; Rahman, A., Ed.; Elsevier Science Publishers: Amsterdam, The Netherlands, 1990; Volume 7, pp. 265–316.
3. Kalinin, V.I.; Silchenko, A.S.; Avilov, S.A.; Stonik, V.A. Progress in the studies of triterpene glycosides from sea cucumbers (Holothuroidea, Echinodermata) between 2017 and 2021. *Nat. Prod. Commun.* **2021**, *16*, 10. [[CrossRef](#)]
4. Silchenko, A.S.; Avilov, S.A.; Kalinin, V.I. Separation procedures for complicated mixtures of sea cucumber triterpene glycosides with isolation of individual glycosides, their comparison with HPLC/MS metabolomic approach, and biosynthetic interpretation of the obtained structural data. In *Studies in Natural Products Chemistry*; Rahman, A., Ed.; Elsevier Science B.V.: Amsterdam, The Netherlands, 2022; Volume 72, pp. 103–146. [[CrossRef](#)]
5. Silchenko, A.S.; Kalinovskiy, A.I.; Avilov, S.A.; Popov, R.S.; Dmitrenok, P.S.; Chingizova, E.A.; Menchinskaya, E.S.; Panina, E.G.; Stepanov, V.G.; Kalinin, V.I.; et al. Djakonoviosides A, A₁, A₂, B₁–B₄—Triterpene monosulfated tetra- and pentaosides from the sea cucumber *Cucumaria djakonovi*: The first finding of a hemiketal fragment in the aglycones; activity against human breast cancer cell lines. *Int. J. Mol. Sci.* **2023**, *24*, 11128. [[CrossRef](#)]
6. Van Dyck, S.; Flammang, P.; Meriaux, C.; Bonnel, D.; Salzet, M.; Fourmier, I.; Wisztorski, M. Localization of secondary metabolites in marine invertebrates: Contribution of MALDI MSI for the study of saponins in Cuvierian tubules of *H. forskali*. *PLoS ONE* **2010**, *5*, 11. [[CrossRef](#)] [[PubMed](#)]
7. Van Dyck, S.; Caulier, G.; Todeso, M.; Gebraux, P.; Fournier, I.; Wisztorski, M.; Flammang, P. The triterpene glycosides of *Holothuria forskali*: Usefulness and efficiency as a chemical defense mechanism against predatory fish. *J. Exp. Biol.* **2011**, *214*, 1347–1356. [[CrossRef](#)] [[PubMed](#)]
8. Van Dyck, S.; Gebraux, P.; Flammang, P. Qualitative and quantitative saponin contents in five sea cucumbers from Indian Ocean. *Mar. Drugs* **2010**, *8*, 173–189. [[CrossRef](#)]
9. Bahrami, Y.; Zhang, W.; Franco, C.M.M. Distribution of saponins in the sea cucumber *Holothuria lessona*; the body wall versus the viscera, and their biological activities. *Mar. Drugs* **2018**, *16*, 423. [[CrossRef](#)]
10. Popov, R.S.; Ivanchina, N.V.; Silchenko, A.S.; Avilov, S.A.; Kalinin, V.I.; Dolmatov, I.Y.; Stonik, V.A.; Dmitrenok, P.S. Metabolite profiling of triterpene glycosides of the Far Eastern sea cucumber *Eupentacta fraudatrix* and their distribution in various body components using LC-ESI QTOF-MS. *Mar. Drugs* **2017**, *15*, 302. [[CrossRef](#)] [[PubMed](#)]
11. Aminin, D.L.; Menchinskaya, E.S.; Pislugin, E.A.; Silchenko, A.S.; Avilov, S.A.; Kalinin, V.I. Sea cucumber triterpene glycosides as anticancer agents. In *Studies in Natural Product Chemistry*; Rahman, A., Ed.; Elsevier B.V.: Amsterdam, The Netherlands, 2016; Volume 49, pp. 55–105.
12. Careaga, V.P.; Maier, M.S. Cytotoxic triterpene glycosides from sea cucumbers. In *Handbook of Anticancer Drugs from Marine Origin*; Kim, S.-K., Ed.; Springer International Publishing: Cham, Switzerland, 2015; pp. 515–528.
13. Aminin, D.L.; Chaykina, E.L.; Agafonova, I.G.; Avilov, S.A.; Kalinin, V.I.; Stonik, V.A. Antitumor activity of the immunomodulatory lead Cumaside. *Int. Immunopharmacol.* **2010**, *10*, 648–654. [[CrossRef](#)]

14. Avilov, S.A.; Kalinin, V.I.; Smirnov, A.V. Use of triterpene glycosides for resolving taxonomic problems in the sea cucumber genus *Cucumaria* (Holothurioidea, Echinodermata). *Biochem. Syst. Ecol.* **2004**, *32*, 715–733. [[CrossRef](#)]
15. Zelepuga, E.A.; Silchenko, A.S.; Avilov, S.A.; Kalinin, V.I. Structure-activity relationships of holothuroid's triterpene glycosides and some in silico insights obtained by molecular dynamics study on the mechanisms of their membranolytic action. *Mar. Drugs* **2021**, *19*, 604. [[CrossRef](#)] [[PubMed](#)]
16. Avilov, S.A.; Kalinovskii, A.I. New triterpene aglycone from the holothurian *Duasmiodactyla kurilensis*. *Chem. Nat. Compd.* **1989**, *25*, 309–311. [[CrossRef](#)]
17. Silchenko, A.S.; Avilov, S.A.; Kalinovskiy, A.I.; Dmitrenok, P.S.; Kalinin, V.I.; Morre, J.; Deinzer, M.L.; Woodward, C.; Collin, P.D. Glycosides from the North Atlantic sea cucumber *Cucumaria frondosa* V—Structures of five new minor trisulfated triterpene oligoglycosides, frondosides A₇-1, A₇-3, A₇-4, and isofrondoside C. *Can. J. Chem.* **2007**, *85*, 626–636. [[CrossRef](#)]
18. Silchenko, A.S.; Avilov, S.A.; Kalinin, V.I.; Stonik, V.A.; Kalinovskiy, A.I.; Dmitrenok, P.S.; Stepanov, V.G. Monosulfated triterpene glycosides from *Cucumaria okhotsensis* Levin et Stepanov, a new species of sea cucumbers from Sea of Okhotsk. *Russ. J. Bioorg. Chem.* **2007**, *33*, 73–82. [[CrossRef](#)]
19. Avilov, S.A.; Antonov, A.S.; Silchenko, A.S.; Kalinin, V.I.; Kalinovskiy, A.I.; Dmitrenok, P.S.; Stonik, V.A.; Riguera, R.; Jimenes, C. Triterpene glycosides from the Far Eastern sea cucumber *Cucumaria conicospermium*. *J. Nat. Prod.* **2003**, *66*, 910–916. [[CrossRef](#)]
20. Silchenko, A.S.; Avilov, S.A.; Antonov, A.S.; Kalinovskiy, A.I.; Dmitrenok, P.S.; Kalinin, V.I.; Stonik, V.A.; Woodward, C.; Collin, P.D. Glycosides from the sea cucumber *Cucumaria frondosa* III. Structure of frondosides A₂-1, A₂-2, A₂-3 and A₂-6, four new minor monosulfated triterpene glycosides. *Can. J. Chem.* **2005**, *83*, 21–27. [[CrossRef](#)]
21. Avilov, S.A.; Kalinovskiy, A.I.; Kalinin, V.I.; Stonik, V.A.; Riguera, R.; Jimenez, C. Koreoside A, a new nonholostane triterpene glycoside from the sea cucumber *Cucumaria koraiensis*. *J. Nat. Prod.* **1997**, *60*, 808–810. [[CrossRef](#)]
22. *Molecular Operating Environment (MOE)*, version 2020.09; Chemical Computing Group ULC: Montreal, QC, Canada, 2020.
23. Gerber, P.R. Charge distribution from a simple molecular orbital type calculation and non-bonding interaction terms in the force field MAB. *J. Comput. Aided Mol. Des.* **1998**, *12*, 37–51. [[CrossRef](#)] [[PubMed](#)]
24. Wildman, S.A.; Crippen, G.M. Prediction of physiochemical parameters by atomic contributions. *J. Chem. Inf. Comput. Sci.* **1999**, *39*, 868–873. [[CrossRef](#)]
25. Drozdova, O.A.; Avilov, S.A.; Kalinovskii, A.I.; Stonik, A.V. Minor glycoside from the holothurian *Cucumaria japonica*. *Chem. Nat. Compd.* **1992**, *28*, 520–521. [[CrossRef](#)]
26. Avilov, S.A.; Kalinovskii, A.I.; Stonik, V.A. New triterpene glycoside from the holothurian *Neothyonidium magnum*. *Chem. Nat. Compd.* **1990**, *26*, 42–45. [[CrossRef](#)]
27. Bonnard, I.; Rinehart, K.L. Thyonosides A and B, two new saponins isolated from the holothurian *Thyone aurea*. *Tetrahedron* **2004**, *60*, 2987–2992. [[CrossRef](#)]
28. Tong, Y.; Zhang, X.; Tian, F.; Yi, Y.; Xu, Q.; Li, L.; Tong, L.; Lin, L.; Ding, J. Philinopside A, a novel marine-derived compound possessing dual anti-angiogenic and anti-tumor effects. *Int. J. Cancer* **2005**, *114*, 843–853. [[CrossRef](#)] [[PubMed](#)]
29. Zhang, S.-Y.; Yi, Y.-H.; Tang, H.-F.; Li, L.; Sun, P.; Wu, J. Two new bioactive triterpene glycosides from the sea cucumber *Pseudocolochirus violaceus*. *J. Asian Nat. Prod. Res.* **2006**, *8*, 1–8. [[CrossRef](#)]
30. Silchenko, A.S.; Kalinovskiy, A.I.; Avilov, S.A.; Andriyaschenko, P.V.; Dmitrenok, P.S.; Kalinin, V.I.; Yurchenko, E.A.; Dautov, S.S. Structures of violaceosides C, D, E and G, sulfated triterpene glycosides from the sea cucumber *Pseudocolochirus violaceus* (Cucumariidae, Denrochirotida). *Nat. Prod. Commun.* **2014**, *9*, 391–399. [[PubMed](#)]
31. Yang, W.-S.; Qi, X.-R.; Xu, Q.-Z.; Yuan, C.-H.; Yi, Y.-H.; Tang, H.-F.; Shen, L.; Han, H. A new sulfated triterpene glycoside from the sea cucumber *Colochirus quadrangularis*, and evaluation of its antifungal, antitumor and immunomodulatory activities. *Bioorg. Med. Chem.* **2021**, *41*, 116188. [[CrossRef](#)] [[PubMed](#)]
32. Silchenko, A.S.; Kalinovskiy, A.I.; Avilov, S.A.; Andriyaschenko, P.V.; Popov, R.S.; Dmitrenok, P.S.; Chingizova, E.A.; Ermakova, S.P.; Malyarenko, O.S.; Dautov, S.S.; et al. Structures and bioactivities of quadrangularisides A, A₁, B, B₁, B₂, C, C₁, D, D₁–D₄, and E from the sea cucumber *Colochirus quadrangularis*: The first discovery of the glycosides, sulfated by C-4 of the terminal 3-O-methylglucose residue. Synergetic effect on colony formation of tumor HT-29 cells of these glycosides with radioactive irradiation. *Mar. Drugs* **2020**, *18*, 394. [[CrossRef](#)] [[PubMed](#)]
33. Maier, M.S.; Roccatagliata, A.J.; Kurriss, A.; Chludil, H.; Seldes, A.M.; Pujol, C.A.; Damonte, E.B. Two new cytotoxic and virucidal trisulfated glycosides from the Antarctic sea cucumber *Staurocucumis liouvillei*. *J. Nat. Prod.* **2001**, *64*, 732–736. [[CrossRef](#)] [[PubMed](#)]
34. Drozdova, O.A.; Avilov, S.A.; Kalinovskii, A.I.; Stonik, V.A.; Mil'grom, Y.M.; Rashkes, Y.V. New glycosides from the holothurian *Cucumaria japonica*. *Chem. Nat. Compd.* **1993**, *29*, 200–205. [[CrossRef](#)]
35. Silchenko, A.S.; Avilov, S.A.; Andriyaschenko, P.V.; Popov, R.S.; Chingizova, E.A.; Dmitrenok, P.S.; Kalinovskiy, A.I.; Rasin, A.B.; Kalinin, V.I. Structures and biologic activity of chitonoidosides I, J, K, K₁ and L—Triterpene di-, tri- and tetrasulfated hexaosides from the sea cucumber *Psolus chitonoides*. *Mar. Drugs* **2022**, *20*, 369. [[CrossRef](#)]
36. Isaeva, M.P.; Likhatskaya, G.N.; Guzev, K.V.; Baldaev, S.N.; Bystritskaya, E.P.; Stonik, V.A. Molecular cloning of sea cucumber oxidosqualene cyclases. *Vestn. FEB RAS* **2018**, *6*, 84–85.
37. Liu, H.; Kong, X.; Chen, J.; Zhang, H. De novo sequencing and transcriptome analysis of *Stichopus horrens* to reveal genes related to biosynthesis of triterpenoids. *Aquaculture* **2018**, *491*, 358–367. [[CrossRef](#)]

38. Li, Y.; Wang, R.; Xun, X.; Wang, J.; Bao, L.; Thimmappa, R.; Ding, J.; Jiang, J.; Zhang, L.; Li, T.; et al. Sea cucumber genome provides insights into saponin biosynthesis and aestivation regulation. *Cell Discov.* **2018**, *4*, 29. [[CrossRef](#)] [[PubMed](#)]
39. Findlay, J.; Daljeet, A.; Matsoukas, J.; Moharir, Y.E. Constituents of the sea cucumber *Cucumaria frondosa*. *J. Nat. Prod.* **1984**, *47*, 560. [[CrossRef](#)]
40. Kalinovskaya, N.I.; Kalinovskiy, A.I.; Kuznetsova, T.A.; Stonik, V.A.; Elyakov, G.B. Uncommon steroidal alcohol from the sea cucumber *Cucumaria japonica*. *Dokl. AN SSSR* **1984**, *278*, 629–633.
41. Makarieva, T.N.; Stonik, V.A.; Kapustina, I.I.; Boguslavsky, V.M.; Dmitrenok, A.S.; Kalinin, V.I.; Cordeiro, M.L.; Djerassi, C. Biosynthetic studies of marine lipids. 42. Biosynthesis of steroid and triterpenoid metabolites in the sea cucumber *Eupentacta fraudatrix*. *Steroids* **1993**, *58*, 508–517. [[CrossRef](#)]
42. Ambia, K.; Goad, L.J.; Hkycko, S.; Garneau, F.-X.; Belanger, J.; ApSimon, J.W. The sterols of the sea cucumber *Psolus phantapus*. *Comp. Biochem. Physiol.* **1987**, *86B*, 191–192. [[CrossRef](#)]
43. Goad, L.J.; Garneau, F.-X.; Simard, J.-L.; ApSimon, J.W.; Girard, M. Isolation of $\Delta^{9(11)}$ -sterols from the sea cucumber *Psolus fabricii*. *Tetrahedron Lett.* **1985**, *26*, 3513–3517. [[CrossRef](#)]
44. Girard, M.; Belanger, J.; ApSimon, J.W.; Garneau, F.-X.; Harvey, C.; Brisson, J.-R. Frondoside A—A novel triterpene glycoside from the holothurian *Cucumaria frondosa*. *Can. J. Chem.* **1990**, *68*, 11–18. [[CrossRef](#)]
45. Avilov, S.A.; Kalinin, V.I.; Drozdova, O.A.; Kalinovskii, A.I.; Stonik, V.A.; Gudimova, E.N. Triterpene glycosides from the holothurian *Cucumaria frondosa*. *Chem. Nat. Compd.* **1993**, *29*, 216–218. [[CrossRef](#)]
46. Silchenko, A.S.; Kalinovskiy, A.I.; Avilov, S.A.; Andryjaschenko, P.V.; Dmitrenok, P.S.; Yurchenko, E.A.; Ermakova, S.P.; Malyarenko, O.S.; Dolmatov, I.Y.; Kalinin, V.I. Cladolosides C₄, D₁, D₂, M, M₁, M₂, N and Q, new triterpene glycosides with diverse carbohydrate chains from sea cucumber *Cladolabes schmeltzii*: An uncommon 20,21,22,23,24,25,26,27-okta-nor-lanostane aglycone. The synergism of inhibitory action of non-toxic dose of the glycosides and radioactive irradiation on colony formation of HT-29 cells. *Carb. Res.* **2018**, *468*, 36–44. [[CrossRef](#)]
47. Silchenko, A.S.; Kalinovskiy, A.I.; Avilov, S.A.; Kalinin, V.I.; Andrijaschenko, P.V.; Dmitrenok, P.S.; Popov, R.S.; Chingizova, E.A.; Ermakova, S.P.; Malyarenko, O.S. Structures and bioactivities of six new triterpene glycosides, psolusosides E, F, G, H, H₁ and I and the corrected structure of psolusoside B from the sea cucumber *Psolus fabricii*. *Mar. Drugs* **2019**, *17*, 358. [[CrossRef](#)] [[PubMed](#)]
48. Avilov, S.A.; Stonik, V.A.; Kalinovskiy, A.I. Structure of four new triterpene glycosides from the sea cucumber *Cucumaria japonica*. *Chem. Nat. Compd.* **1990**, *26*, 670–675. [[CrossRef](#)]
49. Zhu, P.; Zhao, N.; Sheng, D.; Hou, J.; Hao, C.; Yang, X.; Zhu, B.; Zhang, S.; Han, Z.; Wei, L.; et al. Inhibition of growth and metastasis of colon cancer by delivering 5-fluorouracil-loaded pluronic P85 copolymer micelles. *Sci. Rep.* **2016**, *6*, 20896. [[CrossRef](#)] [[PubMed](#)]

Disclaimer/Publisher’s Note: The statements, opinions and data contained in all publications are solely those of the individual author(s) and contributor(s) and not of MDPI and/or the editor(s). MDPI and/or the editor(s) disclaim responsibility for any injury to people or property resulting from any ideas, methods, instructions or products referred to in the content.